

**IN-SITU TENSILE DEFORMATION AND SURFACE CHARGING  
CHARACTERIZATION OF HUMAN HAIR WITH ATOMIC FORCE  
MICROSCOPY**

A Thesis

Presented in Partial Fulfillment of the Requirements for  
the Degree of Master of Science in the  
Graduate School of The Ohio State University

By

Indira. P. Seshadri, B.E.

\*\*\*\*\*

The Ohio State University

2008

Master's Examination Committee

Professor Bharat Bhushan, Advisor

Professor Mark Walter

Approved by

---

Advisor

Mechanical Engineering Graduate Program

## ABSTRACT

Strong beautiful hair is universally desired across various cultures. Hence, the ways in which cleaning conditioning, grooming and styling processes affect the strength, feel and manageability of hair is of interest to beauty care science and technology. Human hair is a complex nanocomposite biological fiber. In this thesis, experiments are performed to better understand mechanical and electrical properties of human hair fibers.

Human hair fibers experience tensile forces during many grooming and styling processes. Hence, characterizing the tensile response of human hair fibers is of considerable interest. The effect of tension on human hair is studied using an atomic force microscope (AFM) and a custom built tensile sample stage. The tensile sample stage allows loading a single hair fiber in tension. In the methodology used here, straining of the hair fiber is stopped intermittently and a marked control area is imaged with the AFM at different strains, upto break point. Morphological changes and deformation that occur with increasing strain are studied. Stress strain data is also simultaneously captured by the sample stage. To understand the effect of damage and treatment on hair fibers virgin, chemically damaged, virgin conditioner treated and chemically damaged conditioner treated, Caucasian hair fibers are studied. To understand differences between damaging processes, mechanically damaged hair is also studied and compared to chemically damaged and virgin hair. Hair from different ethnic types is known to have significantly different properties. In order to understand this difference better, the tensile response of virgin Caucasian, Asian and African hair is investigated. The wet tensile

response of hair is particularly important to explain the effect of wet combing and wet styling processes. Also by studying the wet tensile properties, pathways of penetration of water molecules into the hair fiber can be explained. Hence, virgin damaged and treated hair fibers soaked in water are subjected to tension, and a control area is imaged intermittently. While tension experiments are good baseline studies, most grooming processes are not simple tension. In order to better simulate grooming processes, fatigue tests are carried out, where a single hair fiber is subjected to fatigue. The fatigued fiber is then tested and imaged in tension. Mechanisms for all observed results are proposed.

Another property of interest is the surface charge of human hair. Surface charge of hair has a significant effect on manageability, feel, and appearance. For this reason, controlling charge buildup to improve these factors is an important issue in the commercial hair care industry. Previous studies have looked at static charging characteristics of hair on a macroscale. In this study, static charging characteristics of hair are studied on a nanoscale with an AFM. Surface charge is created on hair by rubbing a control area with a voltage biased AFM tip, to which a small voltage bias is applied. The resulting charge distribution is characterized by measuring the surface potential of the control area in situ with Kelvin probe microscopy. The rubbing load is progressively increased, and the effect of this increase on the charge build up is assessed. Virgin, damaged and conditioner treated hair samples are studied, for a better understanding of charge build up and dissipation. Relevant mechanisms are discussed.

## ACKNOWLEDGEMENTS

First, I would like to thank my advisor Dr. Bharat Bhushan, for giving me the opportunity, support, resources and motivating me to be successful in graduate school. I have learned a lot from him both professionally and otherwise and one day hope to be as dedicated, involved and perfect as him in everything I might do.

I would like to thank all my colleagues in the lab, for discussing and helping me out with problems on numerous instances. I owe a lot to my predecessors in the lab. In particular, Mr. Richard Lodge, for taking the trouble and time to teach me everything he knew about atomic force microscopy and hair, with real concern that I should understand and learn and be able to do experiments independently after he left. He selflessly devoted many hours of his graduating quarter to teach me, his busy schedule non-withstanding. I also owe thanks to my predecessor Mr. Carmen LaTorre for a most helpful, systematic and detailed set of lab notes. Many times, when a problem arose, the solution would already be there in his notes. His notes have saved me an amazing amount of time and effort.

I would like to thank my mother Dr. Usha Seshadri, for being there for me always, for supporting and loving me through everything, and for guiding me on every aspect of life. She has stressed on conceptual understanding, scientific thinking and clear writing from since I was a kid, and has instilled these habits in me, which have proven indispensable for my life and especially research. I would also like to thank everyone else in my family for their love and support. Finally I would like to thank Balaji for coming into my life, sharing it and making it a lot lovelier than it was.

## VITA

March 24, 1985 ..... Born – Chennai, India

2006 ..... B.E. Manufacturing  
Engineering, College of Engineering,  
Guindy, Chennai, India

2006 – 2007 ..... University Fellow, The Ohio State  
University , Columbus, OH

2007 – 2008 ..... Graduate Teaching Associate, The  
Ohio State University , Columbus,  
OH

## PUBLICATIONS

1. I. P. Seshadri and B. Bhushan, “In-situ tensile deformation characterization of human hair with atomic force microscopy”, *Acta Mater.* 56, 774-781 (2008).
2. I. P. Seshadri and B. Bhushan, “Effect of ethnicity and treatments on in-situ tensile response and morphology changes of human hair characterized by atomic force microscopy. *Acta Mater.* (in press).
3. I. P. Seshadri and B. Bhushan, “Effect of rubbing load on nanoscale charging characteristics of human hair characterized by AFM based Kelvin probe” (submitted for publication).

## FIELDS OF STUDY

Major Field: Mechanical Engineering

## TABLE OF CONTENTS

<b>Abstract.....</b>	<b>(i)</b>
<b>Acknowledgement.....</b>	<b>(iv)</b>
<b>Vita.....</b>	<b>(vi)</b>

### CHAPTERS

<b>I.</b>	<b>Introduction.....</b>	<b>1</b>
<b>1.1</b>	<b>In-situ tensile deformation characterization.....</b>	<b>4</b>
<b>1.2</b>	<b>Nanoscale charging characterization.....</b>	<b>8</b>
<b>II.</b>	<b>In-situ tensile deformation characterization.....</b>	<b>11</b>
<b>2.1</b>	<b>Experimental techniques.....</b>	<b>11</b>
<b>2.1.1</b>	<b>Hair Samples.....</b>	<b>11</b>
<b>2.1.2</b>	<b>Tensile stage setup.....</b>	<b>12</b>
<b>2.1.3</b>	<b>Tensile experiment procedure.....</b>	<b>13</b>
<b>2.1.4</b>	<b>Soaking experiments.....</b>	<b>15</b>
<b>2.1.5</b>	<b>Fatigue experiments.....</b>	<b>16</b>
<b>2.2</b>	<b>Results and Discussions.....</b>	<b>17</b>
<b>2.2.1</b>	<b>Tensile properties of virgin damaged and treated hair.....</b>	<b>17</b>
<b>2.2.2</b>	<b>Cuticle response to tension.....</b>	<b>19</b>
<b>2.2.3</b>	<b>Effect of damage on tensile response.....</b>	<b>23</b>

2.2.4	Effect of conditioner treatment.....	25
2.2.5	Tensile properties and response of ethnic hair.....	25
2.2.6	Tensile properties and response of soaked hair.....	30
2.2.7	Effect of fatigue on tensile properties and response.....	39
<b>III.</b>	<b>Nanoscale charging characterization.....</b>	<b>45</b>
3.1	Experimental techniques.....	45
3.1.1	Hair samples.....	45
3.1.2	Charging and Kelvin Probe Microscopy.....	46
3.2	Results and discussions.....	50
3.2.1	Charging characteristics of virgin hair.....	50
3.2.2	Effect of damage on charging characteristics.....	53
3.2.3	Effect of conditioner treatment.....	57
4.	Conclusions.....	59
4.1	In-situ tensile deformation characterization.....	59
4.2	Nanoscale charging characterization.....	61
	List of References.....	64
	Appendix A. Shampoo and conditioner treatment procedure.....	68

## LIST OF FIGURES

<b>Figure 1.1</b> SEM images of Caucasian hair at different levels of magnification (LaTorre and Bhushan, 2005).....	1
<b>Figure 1.2</b> Schematic structure of human hair and of outermost surface of hair showing 18-MEA containing lipid layer location (Negri and Cornell, 1993; Robbins, 1994; Smith and Swift, 2002).....	2
<b>Figure 2.1</b> Schematic diagram of the setup used to conduct in situ tensile testing of human hair in AFM.....	12
<b>Figure 2.2</b> Strain and stress cycling used for fatigue tests.....	16
<b>Figure 2.3</b> Stress strain curves showing for five types of hair - Virgin, virgin treated, chemically damaged, chemically damaged treated, mechanically damaged. Transition of alpha keratin to beta keratin is the reason for the unique shape of the curve.....	18
<b>Figure 2.4</b> AFM topographical images and 2-D profiles at indicated planes of a control area showing progress of damage with increasing strain in (a) virgin hair and virgin hair treated with one cycle of commercial conditioner. (b) chemically damaged hair and chemically damaged hair treated with one cycle of conditioner and. (c) mechanically damaged hair. Cuticle lifts off at 20% strain in all cases. Fracture of cuticle outer layer occurs at 20% strain in chemically damaged hair and 10% strain in mechanically damaged hair.....	20
<b>Figure 2.5</b> Schematic of the progress of morphology change in virgin and damaged hair. Top and cross sectional views are shown. In the case of virgin hair, lift off of cuticle	

outer layer is seen. Whereas in damaged hair, both lift off and cuticle fracture is noticed.....24

**Figure 2.6** Stress strain curves for virgin Caucasian, Asian and African hair. Transition from alpha to beta keratin is the reason for the unique shape of these curves.....26

**Figure 2.7** AFM topographical images and 2-D profiles at indicated locations of a control area showing progress of damage with increasing strain in Caucasian, Asian and African hair. Caucasian hair shows cuticle lift of at ~20% and Asian at ~25%. African hair shows cuticle rupture.....29

**Figure 2.8** Stress strain curves for unsoaked and soaked samples of Caucasian virgin, chemically damaged and chemically damaged treated hair and virgin soaked and dried hair.....34

**Figure 2.9** AFM topographical images and 2-D profiles at indicated locations of a control area showing progress of damage with increasing strain in (a) Virgin Caucasian soaked hair and soaked and dried hair, (b) soaked and unsoaked samples of chemically damaged and chemically damaged treated hair. All soaked samples show lift off at about 5% strain. Chemically damaged and damaged treated hair show scale fracture. For treated soaked hair additional cuticles lift off at 20% strain.....35

**Figure 2.10** Schematic diagram of the effect of soaking on hair morphology.....38

**Figure 2.11** Stress strain curves for virgin, chemically damaged and chemically damaged treated Caucasian hair subjected to fatigue. Virgin Caucasian and virgin African stress strain curves are shown for comparison.....40

**Figure 2.12** AFM topographical images and 2-D profiles at indicated locations of a control area during (a) fatigue cycling of virgin Caucasian hair, (b) tensile test of fatigued

virgin Caucasian hair, fatigued chemically damaged Caucasian hair, fatigued chemically damaged and treated Caucasian hair. Fatigued virgin Caucasian hair shows cuticle fracture. Fatigued chemically damaged and chemically damaged treated hair shows cuticle rupture. All hair samples show lift off at ~5 % strain.....42

**Figure 3.1** Schematic of first pass of Kelvin probe technique measuring surface height (Bhushan and Goldade, 2000a); (b) Schematic of second pass of Kelvin probe technique measuring surface potential (Bhushan and Goldade, 2000a); (c) Jumper configuration during surface potential measurement for all data shown.....49

**Figure 3.2** AFM topography images and KPM surface potential maps of virgin hair before and after rubbing with voltage biased tip at two different normal loads. The area where wear and charge deposition was performed is marked on the topography image.....51

**Figure 3.3** Bar chart showing average surface potential change and its dependence on normal load for all the hair samples studied.....53

**Figure 3.4** Topography images and surface potential maps before and after rubbing with voltage biased tip at two different normal loads for (a) chemically damaged hair; (b) chemically damaged hair treated with PDMS silicone conditioner; (c) chemically damaged hair treated with amino silicone conditioner. The area where wear and charge deposition was performed is marked on the topography image.....54

**Figure 3.5** Topography images and surface potential maps before and after rubbing with voltage biased tip for mechanically damaged hair. The area where wear and charge deposition was performed is marked on the topography image.....56

## LIST OF TABLES

<b>Table 2.1</b> Mechanical properties of hair - The values presented here are based on 20 measurements. Values show upto 15% variation from sample to sample.....	19
<b>Table 2.2</b> Mechanical properties of ethnic hair - The values presented here are based on 15 measurements. Values show upto 15% variation from sample to sample.....	27
<b>Table 2.3</b> Mechanical properties of unsoaked and soaked hair. All values are based on 15 measurements. data shows a 15% variation sample to sample.....	31
<b>Table 2.4</b> Mechanical properties of fatigued hair - The values presented here are based on 5 measurements. Values show upto 15% variation from sample to sample.....	41
<b>Table 2.5</b> Summary of failure modes of various hair samples.....	44

## CHAPTER 1

### INTRODUCTION

Healthy, beautiful and strong hair is desired universally. Human hair is a complex nanocomposite fiber whose physical appearance, mechanical strength and chemical properties are governed by a variety of factors like ethnicity, cleaning, grooming, chemical treatments and environment. While the surface of hair appears smooth and glossy to the naked eye, under high magnification it is covered with a structure of scales known as cuticles. Figure 1.1 shows scanning electron microscope (SEM) images of Caucasian hair at two levels of magnification (LaTorre and Bhushan, 2005a). The scaled cuticular structure of hair is evident. Chemically, the major constituent of hair is the protein keratin (Zviak, 1986; Robbins, 1994; Feughelman, 1997; Jolles *et al.*, 1997; Morioka, 2005; Bhushan and LaTorre, 2008). Like other proteins, keratin is a condensation polymer of amino acids. The major percentage of amino acid chains in keratin are cystine chains. The inter chain and intra chain disulfide bonds of cystine are responsible for the mechanical strength of hair.

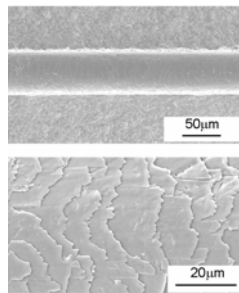


**Figure 1.1** SEM images of Caucasian hair at different levels of magnification (LaTorre and Bhushan, 2005).

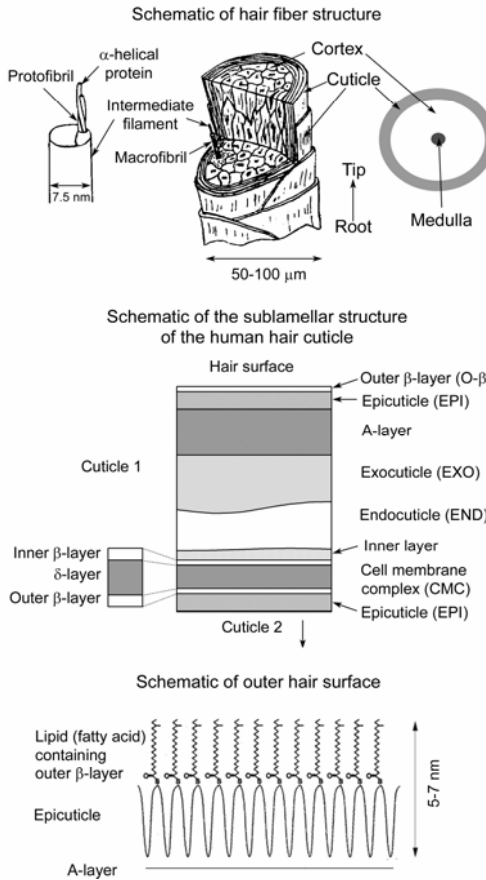


**Figure 1.2** Schematic structure of human hair and of outermost surface of hair showing 18-MEA containing lipid layer location (Negri and Cornell, 1993; Robbins, 1994; Smith and Swift, 2002).

The two main structural components of hair are the cuticle and the cortex. The cortex is the main bulk of the fiber. Figure 1.2 shows the internal structure of a cortical cell, consisting of a matrix in which intermediate filaments are embedded. The intermediate filament consists of the protofibril that makes up the crystalline alpha helical keratin filament. The cuticle is the outermost layer that protects the cortex. It consists of flat overlapping cells (scales) that are attached to the root or proximal end and point towards the tip or distal end of the fiber. Each cuticle cell is 0.3 to 0.5  $\mu\text{m}$  thick and the visible length is anywhere between 5 to 10  $\mu\text{m}$ . In human hair, the cuticle layer is

generally around 10 scales thick. Each cuticle cell consists of sublamellar layers: the epicuticle, the A layer, exocuticle, endocuticle and the inner layer. These layers vary markedly in their cystine content. The epicuticle is the cell membrane of the cuticle cell. The A layer and the exocuticle are rich in cystine content (~30% and ~15% respectively) highly cross linked and mechanically strong. The endocuticle is low in cystine content (~3%) and weak mechanically. The cell membrane complex is the intercellular cement that holds the cuticle cells together. It is again a lamellar structure consisting of the outer  $\beta$ -layer  $\delta$ -layer and inner  $\beta$ -layer. Attached to the epicuticle, or the outermost layer of the cuticle cell, is the outer  $\beta$  lipid layer, which is also part of the cell membrane complex. This layer is made up fatty acids, mainly 18-methyleicosanoic acid (18-MEA). This layer is important in that it gives hair its lubricity and hydrophobic nature. In the case of chemical or mechanical damage to hair, it is stripped away, rendering a rough feel to the hair surface (Kamath *et al.*, 1978; Negri and Cornell, 1993; Lodge and Bhushan, 2006a, b; LaTorre and Bhushan, 2005). Sometimes, a third structure of cells may be present as the inner core of hair. This structure is known as the medulla, and is absent in some hair types such as extremely fine hair or blonde hair (Robbins, 1994).

Two different studies have been carried out in this thesis to characterize human hair fibers, in-situ tensile response characterization and nanoscale charging characterization. These studies are described in detail in the next sections.

## **1.1 In-situ tensile deformation characterization**

An important indicator of hair health and strength, as perceived commonly, is its resistance to fracture or breakage. The first part of this thesis concentrates on the tensile response of hair fibers and how this response changes for various different types of hair. Hair fibers are stressed as they are combed, styled, groomed and treated in day to day life. The understanding of the behavior of hair fibers under these tensile stresses, is hence of great interest to the beauty care industry. Most previous studies and theoretical modeling of the tensile properties of hair and other keratin fibers have concentrated on the response of the cortex (Kreplak *et al.*, 2002; Akkermans and Warren, 2004). However, from a cosmetic point of view, it is the cuticle that gives hair a healthy or unhealthy look. Most beauty care products and treatments primarily affect the cuticle layers. Also day to day grooming and styling processes predominantly damage the cuticle layers (Chen and Bhushan, 2005; LaTorre and Bhushan, 2005b). Hence a better understanding of the cuticular response to tensile stress is very important.

Atomic force microscopy (AFM), over the past few years has emerged as a viable tool to study hair surface structure, specially the cuticular structure at the nanometer scale. Its major advantages over traditional SEM include the absence for the need for special sample preparation procedures and the capability to perform in situ experiments (Bhushan, 2002). In situ surface characterization of deformation with AFM has been carried out on materials like binary aluminum alloys, polymeric thin films and magnetic tapes in the past (Tong *et al.*, 1997; Bobji and Bhushan, 2001a, b; Tambe and Bhushan, 2004). With in-situ experiments it is possible to systematically follow the progress of morphological change and deformation in the material, and to accurately pinpoint the

initiation of major deformation events. On human hair, characterization of fracture after deformation has been carried out using SEM and light/fluorescence microscopy (Henderson *et al.*, 1978; Swift, 1999). In-situ experiments on deformation progress in human hair subjected to tensile loading have not been carried out before.

Hence, the objective of this study is to develop and implement an AFM based technique to study in-situ, the response of the human hair fiber, specifically the surface cuticle structure to tensile loading. Tests were conducted on both virgin and damaged hair samples, in order to study the difference in response between healthy and weakened cuticle cells. Differences between chemical damage arising from processes like bleaching and coloring and mechanical damage to the cuticle layers was also compared. The strain levels experienced by hair fibers are typically less than 5% during combing/detangling and less than 12% during styling (Zviak, 1986; Robbins, 1994). In isolated cases hair fibers can also break, especially during detangling. In order to fully understand the deformation process of the cuticle, the fiber is strained to the break point in this study.

Conditioners are hair care products that are very commonly used by consumers. Conditioners form a thin coating on the hair and can cause changes to the tribological properties of the cuticle surface. Conditioner consists of a gel network chassis (cationic surfactant, fatty alcohols and water) for superior wet feel and a combination of conditioning actives (silicones, fatty alcohols and cationic surfactant) for superior dry feel. Cationic surfactants are critical to the forming of the lamellar gel network in conditioner, and also act as a lubricant and static control agent, since their positive charge aids in counteracting the negative charge of the hair fibers. The cationic surfactants in the conditioners used in this study are quaternary amine based surfactants. They have a low

energy alkyl chain on one end of the molecule and relatively higher energy cationic group on the other. Fatty alcohols are used to lubricate and moisturize the hair surface, along with forming the gel network. Among all the components of conditioner, silicones are the main source of lubrication for dry hair. Conditioners create a smooth soft feel for the consumer and protect the cuticle layer from further wear. Hence it is also of interest to ascertain if conditioner plays any part in the tensile response of the hair fiber. Both virgin hair and chemically damaged hair samples treated with one cycle of commercial conditioner were tested in the present study.

Ethnicity is an important factor while determining formulations for beauty care products. This is because different ethnic hair types are significantly different in their structure and properties. Hair falls under three main ethnic types - Caucasian, Asian and African. Asian hair is found to have the maximum strength and diameter followed by Caucasian hair. Both these hair types have a predominantly circular cross section. African hair is generally more liable to damage and breakage, has lesser moisture content than Asian or Caucasian hair and has a highly elliptical cross section. Asian hair is generally very straight along its axis, Caucasian hair varies from straight to wavy to moderately curly. African hair however exhibits a characteristic tightly curled structure (Wei *et al.*, 2005). Chemically all ethnic hair are found to have the same protein structure and composition (Menkart *et al.*, 1984; Dekoi and Jedoi, 1988, 1990). These variations in shape (diameter, ellipticity, and curliness) of hair from different ethnic origins depend on several factors, including the shape of the hair follicle and its opening; these vary from one person to another and also between races (Gray, 2001; Thibaut *et al.*, 2005). The pronounced ellipsoidal cross-section of hair shaft in African hair could be caused by a

heterogeneous and asymmetric fiber framework, in addition to internal mechanical stresses (Thibaut and Bernard, 2005). Previously, it was thought that elliptical cross section of hair is responsible for curl. While circular cross sections (Asian and Caucasian) generally have straight hair, curly hair has a predominantly elliptical cross section (African). However, recent studies suggest that hair follicle shape and not the cross section is responsible for hair curl (Thibaut *et al.*, 2005). This means that if the follicle is straight, even an elliptical cross section could give rise to straight hair. Both *in-vitro* growth studies and computer aided three dimensional reconstruction (Lindelof *et al.*, 1988) support this claim. Curvature of the curly hair is programmed from the basal area of follicle. This bending process is apparently linked to a lack of symmetry in the lower part of the bulb, affecting the hair shaft cuticle. In this study, the surface morphology changes of the three types of ethnic hair fibers under tension are compared. These are then correlated to known properties of these hair types.

Water and water vapor significantly affect tensile properties of human hair. Human hair reaches equilibrium in water and exhibits diametrical swelling of up to 16% (Robbins, 1994). Studying the mechanism of penetration of water into the hair fiber, and the pathway of water molecules is important for processes like dyeing and treatment with hydrolyzed products (Swift *et al.*, 2000). Also the effect of tensile forces on hair, while it is in a wet state is important to assess effects of wet combing and wet styling processes. In this study hair fibers soaked in de-ionized (DI) water are subjected to stretching and the changes in surface morphology are observed. Conditioners are hair care products that are very commonly used by consumers. These consist of a gel network chassis(cationic surfactant, fatty alcohol and water) for superior wet feel and a combination of

conditioning additives (silicones, fatty alcohols and cationic surfactant) for superior dry feel (LaTorre *et al.*, 2006 ). As discussed earlier, conditioners form a thin coating on the hair and can cause changes to the tribological properties of the cuticle surface. They are also thought to influence water penetration into the fiber (Wei *et al.*, 2005). To study variation in the penetration of water molecules into the fiber with damage and treatment, chemically damaged and soaked, and chemically damaged samples treated with commercial conditioner and soaked are studied. These are compared to the dry tensile response of the corresponding hair types.

Many real life grooming processes like combing and styling are more than simple tension, they are generally fatigue processes, where the stress on the hair fiber varies in cycles. Hence it is interesting to study the effect of fatigue on the hair fiber. Here, virgin, chemically damaged and conditioner treated hair fibers are subjected to a fixed number of cycles of fatigue loading. After this, a tension test is carried out on the fiber. These results are then compared with non-fatigued fibers and the effect of fatigue is assessed.

## **1.2 Nanoscale charging characterization**

Hair has a tendency to develop static charge when rubbed with dissimilar materials like latex, human skin, plastic etc. Human hair is a good insulator with an extremely high electrical resistance. Electrical resistance of human hair fibers has been measured in previous studies by applying a voltage and measuring voltage drop across a resistor in series with the fiber, using a high sensitivity electrometer (Grady and Hersh, 1977; Hersh *et. al.*, 1981). The resistance per unit length of the fiber was found be on the order of  $10^{18}$  ohm/cm. Due to this high resistance, charge on hair is not easily dissipated, especially in dry environments. This causes repulsion between hair fibers, and

consequent lack of manageability and static flyaway effects. Systematically studying the production of charge on the hair surface, and accurately measuring surface charge, is hence highly beneficial. Many macroscale studies have looked at the static charging of human hair (Mills *et. al.*, 1956; Barber and Posner, 1958; Lunn and Evans, 1977; Jachowicz *et. al.*, 1985). Most of these studies consist of rubbing hair bundles with various materials like plastic combs, Teflon, latex balloons, nylon, and metals like gold, stainless steel and aluminum. Hair in these cases is charged by a macroscale triboelectric interaction between the surface and the rubbing element. The kinetics of the charging process and the resulting charge are then measured using modified electrometers. While these studies give a macroscale overall indication, the actual charging occurs at a much smaller scale, at the contact sites between individual hair fibers and the rubbing element.

In a few recent studies AFM based Kelvin probe microscopy has been used to characterize charging of human hair. AFM based KPM is a widely applied technique, which has been used for high resolution measurements of surface potential, of a variety of conducting, insulating and semi conducting surfaces (DeVecchio and Bhushan 1998; Bhushan and Goldale, 2000a, b; Schroeder, 2006). KPM has been used to characterize charge transport on hair surface, by applying a voltage gradient across hair surface and then measuring the resulting potential (Lodge and Bhushan, 2007a). Triboelectric charging of hair has also been investigated, by rubbing hair manually with a latex finger cot and then measuring the resulting potential (Lodge and Bhushan, 2007b). In these cases, the charge measurement technique - KPM, is nanoscale. However, the rubbing process or charge production process is macroscale. In a macroscale rubbing process, it is very difficult to control the rubbing load and the rubbing area. The area where contact or

charging occurred may not be the area where potential is measured. Also there may be significant mass transfer. Hence for systematically studying charging characteristics, it is essential to charge hair surface on a nanoscale by a controlled process.

In the present study, hair surface is charged by rubbing a control area with a conductive metal coated Atomic Force Microscope (AFM) tip, biased with a low DC voltage. The resulting potential over this area is then measured in situ with KPM. As discussed in a later section, the low DC tip bias of 6V was found necessary to produce a consistent potential contrast over the rubbed area. Also, the value of this DC bias was kept constant at 6V through all experiments in this study. Hence, any difference in measured surface potential arises from either the nature of treatments on the hair surface, or the parameters of the rubbing process. The parameter of the rubbing process that is likely to have the most effect, and is also most difficult to control in macroscale experiments, is the rubbing load. To study the effect of rubbing load, the load during the charging process is progressively increased. Potential measurements are taken before and after rubbing at each load.

To assess the effect of damaging treatments, hair that has been chemically damaged by bleaching and coloring, and hair that has been mechanically damaged by combing are studied. Conditioners are commonly used products that are known to improve the feel of hair surface, by a reduction of friction. They are also thought to possess static charge control properties. In order to study this effect, hair treated with two types of conditioners - a commercial polydimethylsiloxane (PDMS) silicone based conditioner and a newer amino silicone based conditioner is studied.

## CHAPTER 2

### IN-SITU TENSILE DEFORMATION CHARACTERIZATION

#### 2.1 Experimental techniques

##### 2.1.1 Hair samples

Hair samples were received from Procter & Gamble (Cincinnati, OH) and prepared per Appendix A. Four main categories of hair samples were studied in this portion of the thesis: virgin, chemically damaged, mechanically damaged and treated. Virgin samples are specimens that have no signs of chemical damage. Chemically damaged hair fibers have been bleached and colored, which are representative of common hair alteration methods. Mechanically damaged hair fibers were exposed to combing to cause mechanical damage, and were observed under an optical microscope at 100x and found to exhibit a high degree of cuticle damage. Treated samples have been treated with one cycle of a Procter & Gamble commercial conditioner containing polydimethylsiloxane (PDMS) silicone. All hair samples had undergone two rinse/wash cycles of commercial shampoo treatment (in the case of treated samples, prior to conditioner treatments). The samples of interest in this portion of the thesis are Caucasian virgin, Asian virgin, African virgin, Caucasian virgin treated, Caucasian chemically damaged, Caucasian chemically damaged treated and Caucasian mechanically damaged.

The samples arrived as hair swatches approximately 0.3 m long. Although the exact location from the root is unknown, it is estimated that hair samples used for testing were between 0.1 and 0.2 m from the scalp. The tests were conducted on hair segments 38 mm long taken approximately from the middle parts of hair samples.

### 2.1.2 Tensile stage setup

In-situ tensile tests of human hair fibers in an AFM were conducted using a custom-built tensile stage that attaches to the AFM base and uses a linear stepper motor to load a single hair fiber in tension. The AFM used was a commercial system (Dimension 3100, Digital Instruments, Santa Barbara, CA). Figure 2.1 shows a schematic of the stage used in place of the regular AFM sample holder.

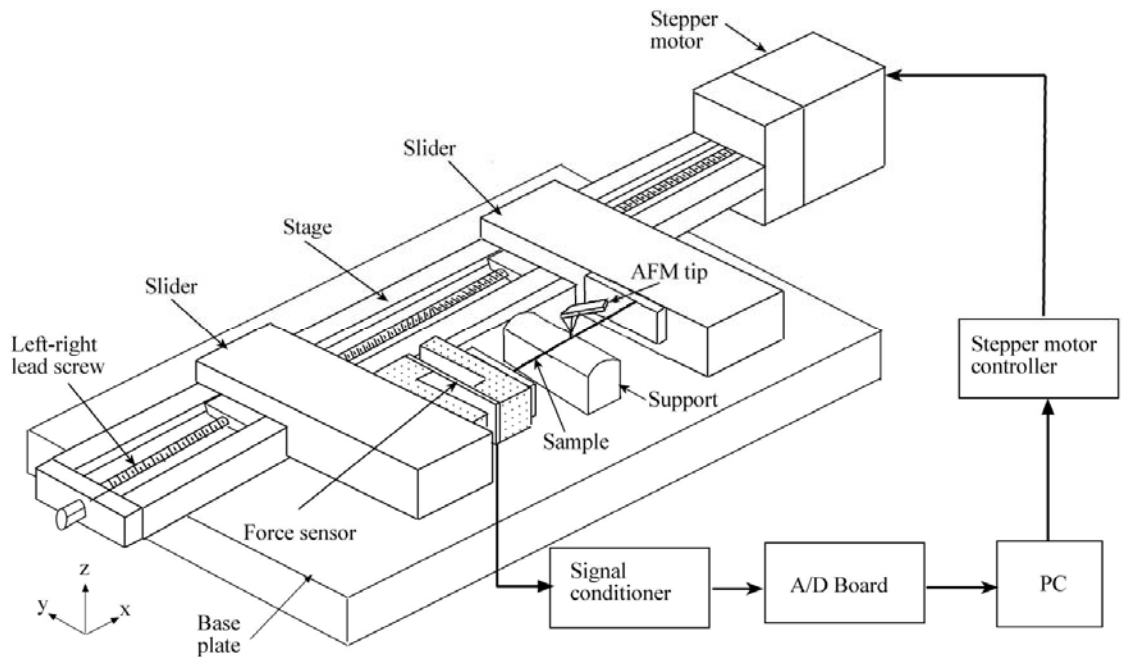


**Figure 2.1** Schematic diagram of the setup used to conduct in situ tensile testing of human hair in AFM.

During scanning, the sample is held stationary while the cantilever tip mounted on an X-Y-Z piezo, moves back and forth. The hair sample is firmly clamped in between two sliders to prevent slipping on load application. Stage motion is achieved by a left-right combination lead screw that keeps the sample at approximately the same position with respect to the scanning tip. This helps in locating the same control area after each loading increment is applied. A 40 TPI pitch lead screw in combination with 400 steps per revolution stepper motor (model PX245 – 01AA, using the controller NF-90, both from Velmex Inc) gives a minimum displacement of 1.6  $\mu\text{m}$ . For a sample length of 38 mm (1.5 in), this corresponds to a minimum strain rate of  $8.33 \times 10^{-3}$  % per second. The strain applied was obtained from the total number of steps through which the stepper motor was rotated. The minimum strain rate was used throughout this study. A beam-type strain gauge force sensor (model LCL-010, Omega Engineering Inc., Stamford, CT), with a resolution of 10 mN was used. The corresponding stress was obtained using the diameter of the individual hair fiber, measured using the high resolution optical system of the AFM. This is done because individual hair fibers vary considerably in diameter. The stiffness of the force sensor (18 kN/m) is very high compared to the sample stiffness.

To minimize airborne vibrations during AFM imaging, the hair fiber was supported with an aluminum block having a smooth radius of curvature of 25.4 mm as shown in Fig 3.

### **2.1.3 Tensile experiment procedure**

Hair samples, 38 mm in length, were held between the movable sliders of the stage and axial load was applied using the stepper motor. During the tensile test, the loading was stopped intermittently and the sample was scanned with AFM for changes in morphology. The support block was removed during straining and carefully inserted again while imaging. The tension tests were conducted at a constant strain rate of  $8.33 \times 10^{-3} \%$ . For AFM scanning a 20nm radius, 0.06 N/m silicon nitride cantilever was used in contact mode. The scan size was 25  $\mu\text{m}$  and a scan frequency of 2 Hz was selected. For stress strain curves, data from the load cell was used. All tensile parameters presented in this study are based on about twenty individual measurements.

With every load increment, there was a corresponding increase in length of the hair sample and hence a shift in the location of the control area from its previous position. It was therefore necessary to accurately locate the control area after every load increment before scanning. One of the approaches is to make a set of special markers on the sample by scratching which are big enough to show up in the optics system of the AFM. Using these as guides, the area can be located (Bobji and Bhushan, 2001a, b). However, in the case of hair samples, artificial scratches do not show up in the optics system, because of the non reflective nature of the sample. To locate the same control area in hair, scanning over a rectangular area with high aspect ratio, along with a physical marker (insulation tape) has been used successfully in the past (Breakspeak and Smith, 2003). For the present purposes, a mark was made on the hair sample with commercial nail polish. Nail polish adheres to hair surface firmly, even after many load increments, and does not peel off. Also, because of its reflective nature, it shows up clearly in the optics system of the AFM. The size of the marker was anywhere between a 0.5 mm to 1.5 mm. An area

sufficiently far away (at least 500  $\mu\text{m}$ ) from the marker was chosen to avoid any interference of the marker with the morphology change. The control area was located each time by scanning a high aspect ratio rectangle, in the vicinity of the marker. The required region was then located by multiple zooming and centering, with the AFM itself, and a smaller, square, final area was scanned.

#### **2.1.4 Soaking experiments**

All soaking experiments were carried out by soaking hair fibers in a beaker of DI water for 5 min (Wei *et al.*, 2005, Bhushan *et al.*, 2007). It is known that water penetrates hair in lesser than 15 min, while water vapor takes 18 - 24 h (Robbins, 1994). Also 5 min is a typical exposure time during bathing/ showering. Once soaked the hair fiber is found to retain water for upto 20 min in ambient conditions, and it remains saturated if kept in a **wet** environment (LaTorre *et al.* 2006). The soaked hair fiber was fixed to the tensile stage and the tension experiment was carried out. In most cases the stretching process and acquiring a full set of images of the control area till break point took more than 20 min. Hence, every 20 min, the stretching experiment was stopped, the support removed and a DI water bath was held up to the fiber for 5 min and simultaneously water was dripped on the fiber with a clean piece of sponge. This helped keep the hair fiber wet throughout the experiment. Care was taken not to disturb or make direct contact with the stretched hair fiber during the wetting process.

For the soak and dry experiments, hair soaked for 5 min was taken out of the beaker and allowed to dry in ambient conditions for 3 h. The fiber was then used for tension tests.

### 2.1.5 Fatigue experiments

Fatigue experiments were carried out by controlling and cycling strain, through programming the stepper motor of the tensile stage. Cuticle lift off, the first morphological change during fiber failure, is known to occur at 20% strain (Seshadri and Bhushan, 2008). Hence the maximum strain during fatiguing was kept below that value at 15% strain. The corresponding stress was measured using load values from the load cell as described in an earlier section. Figure 2.2 displays a typical stress/strain cycle. For 15% strain the stress is anywhere between 60 - 80 MPa.

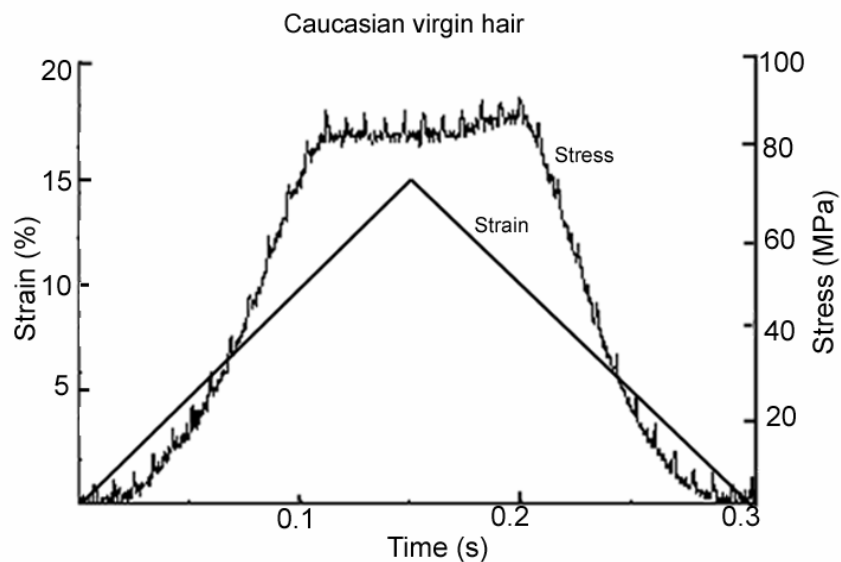


**Figure 2.2** Strain and stress cycling used for fatigue tests

The strain rate used during cycling was 38 mm/sec. A full cycle took 300 ms. Each fiber was subjected to 5000 such cycles. In Fig 2b it is seen that the stress remains at zero for some time at the beginning and end of each cycle. This is because hair fibers undergo some permanent deformation and the stress goes to zero before the strain does. The number of cycles was selected such that most of the hair fibers subjected to fatigue survived the test without breaking. These fibers were then removed and once again fixed to the stage, such that the gauge length was 38mm, and then subjected to a normal tension test. This process was followed so that the data obtained in this experiment would be comparable to tension test data obtained in other experiments in this study.

## **2.2 Results and discussions**

### **2.2.1 Tensile properties of virgin damaged and treated hair**

Figure 2.3 presents stress strain curves virgin hair, virgin treated hair, chemically damaged hair, chemically damaged treated hair and mechanically damaged hair. The stress strain curve of human hair is similar to that of wool and other such keratinous fibers (Zviak, 1986). When a keratin fiber is stretched, the load elongation curve shows three distinct regions as marked in Fig 2.3. In the pre-yield region, also referred to as the Hookean region, stress and strain are proportional, and an elastic modulus can be found. This region is the homogenous response of alpha keratin to stretching. The resistance is provided by hydrogen bonds that are present between turns and stabilize the alpha helix of keratin. The yield region represents transition of keratin from the alpha form to the

beta form, the chains unfold without any resistance, and hence the stress does not vary with strain. The beta configuration again resists stretching. So, in the post-yield region, the stress again increases with strain, till the fiber breaks. This alpha to beta transition of keratin is the reason for the unique shape of the stress strain curve of hair. Typically, yield begins around 5% and post-yield begins at around 15% strain.

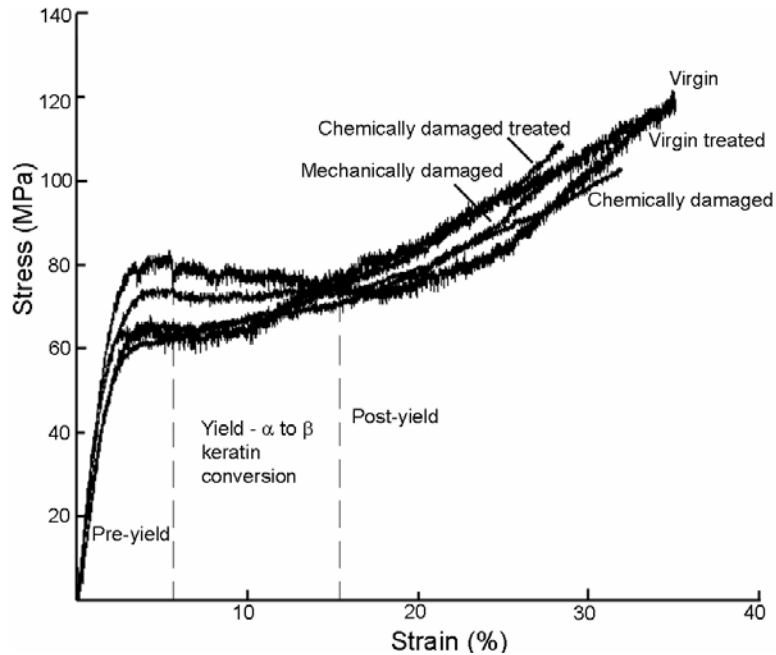


**Figure 2.3** Stress strain curves showing for five types of hair - Virgin, virgin treated, chemically damaged, chemically damaged treated, mechanically damaged. Transition of alpha keratin to beta keratin is the reason for the unique shape of the curve.

Table 2.1 presents the mechanical properties of the various types of hair studied.

Both from the stress strain curves and the mechanical properties, there is no apparent difference in tensile properties of the different hair types. In the dry state, the tensile properties of hair are significantly contributed by the cortex. Hair fibers oxidized with diperisophthalic acid, which causes almost total removal of cuticle, have shown no significant change in mechanical properties (Robbins and Crawford, 1991). In the case of conditioner treatment and mechanical damage, the only change is in the cuticle. Hence, it is logical that the mechanical properties do not have visible change. In the case of

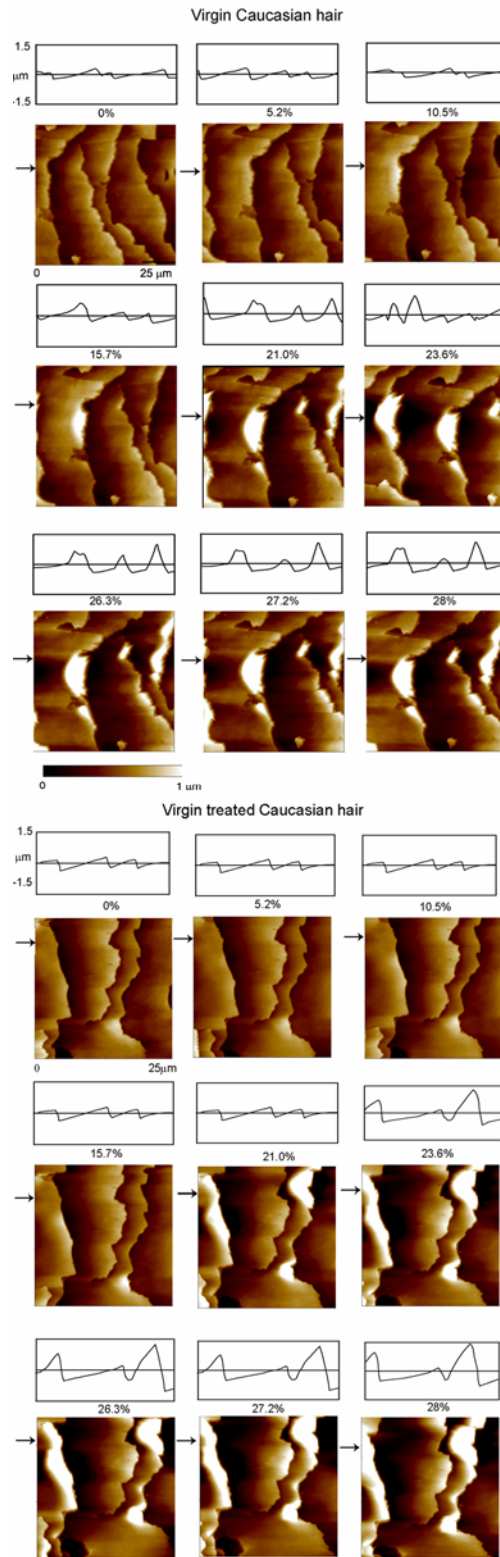
chemical damage, apart from cuticle damage, oxidation of the cystine in keratin to cysteic acid residues occurs, and hence disrupts the disulfide cross links. However, the disulfide bonding does not influence tensile properties of keratin fibers in the dry state.

**Table 2.1** Mechanical properties of hair - The values presented here are based on 20 measurements. Values show upto 15% variation from sample to sample.

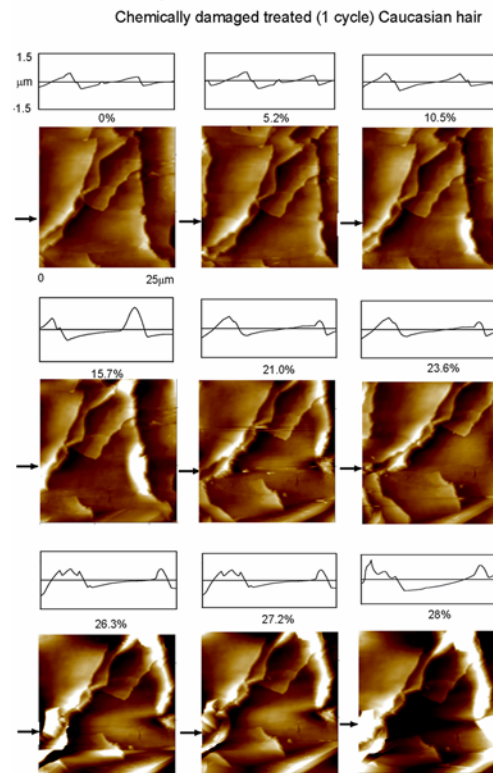
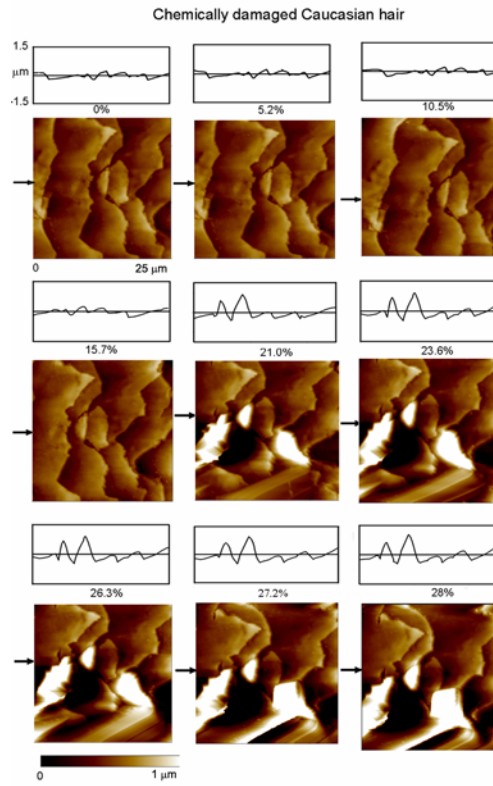
	Virgin	Virgin treated	Chemically damaged	Chemically damaged treated	Mechanically damaged
Elastic modulus (GPa)	3.3	3.7	3.3	2.9	2.6
Yield strength (MPa)	67	75	61	74	64
Breaking strength (MPa)	117	118	107	108	103
Strain at break (%)	35	35	32	31	30

### 2.2.2 Cuticle response to tension

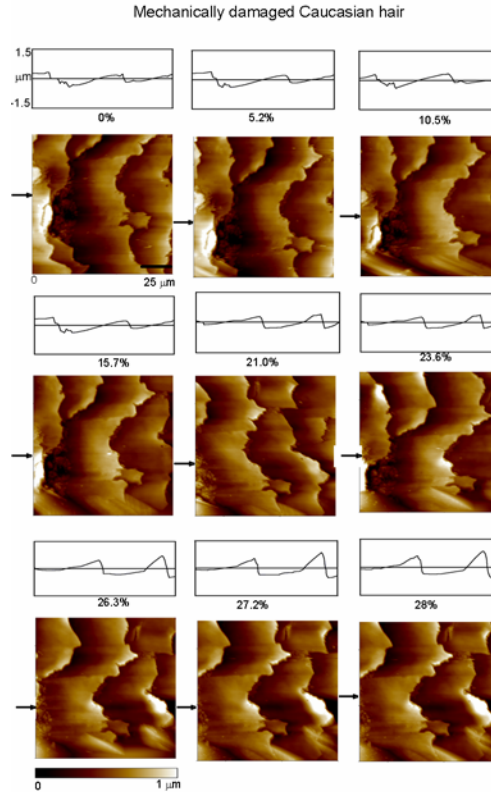
Figure 2.4 shows AFM topographical images, and 2-D profiles at indicated planes, of a given control area with increasing strain of the various types of hair studied. The dominant effect of stretching across all hair types, is seen to be the lifting of the outer cuticle layer with increasing strain.



(a)



(b)



(c)

**Figure 2.4** AFM topographical images and 2-D profiles at indicated planes of a control area showing progress of damage with increasing strain in (a) virgin hair and virgin hair treated with one cycle of commercial conditioner. (b) chemically damaged hair and chemically damaged hair treated with one cycle of conditioner and. (c) mechanically damaged hair. Cuticle lifts off at 20% strain in all cases. Fracture of cuticle outer layer occurs at 20% strain in chemically damaged hair and 10% strain in mechanically damaged hair

In the case of virgin hair (Fig 2.4(a)), this is seen to be the only effect of tension. The cuticle lift off is sudden and occurs consistently at around 20% strain. As mentioned earlier, human hair cuticles have a lamellar structure. The various layers of human hair vary in their cystine content. This causes variation in their mechanical strength. The epicuticle and exocuticle are high in cystine content and are extremely rigid. The endocuticle and cell membrane complex are low in cystine content and are more extensible. Stretching hair sets up interlayer shear forces due to this difference in

extensibility (Reutsch and Weigmann, 1996). At 20% strain delamination occurs, and the inner cuticle layers separate from the outer ones. This causes outer cuticle lift off and hence the change in height and slope observed in the AFM images and corresponding cross sectional profiles.

The top half of Fig 2.5 shows a schematic of the progress of deformation in virgin hair. After the initial lift off at 20%, the cuticle height and slope stays more or less constant till breakage of the hair fiber at 30-35% strain.

### **2.2.3 Effect of damage on tensile response**

Figure 2.4 (b) shows topographical images of chemically damaged hair, while 2.4 (c) presents the same data for mechanically damaged hair. Apart from the lift off discussed earlier, another noticeable effect in both cases is the disappearance of some cuticle edges and the appearance of sponge like scales instead. Sponge like scales in the cuticle have been observed earlier while isolating human hair cuticle from the hair fiber, these are thought to be remains of cuticle cells, which have split upto the endocuticle (Swift and Bews, 1974). Chemical and mechanical damage cause cuticle damage and weakening. Hence in the case of damaged hair, along with failure and delaminations in the endocuticular region, fracture of the outer cuticle occurs to expose the inner cuticle. This shows up as the sponge like scales observed. The bottom half of Fig 2.5 shows a schematic of the progress of damage in damaged hair fibers as against virgin hair.

Comparing mechanical damage and chemical damage, it is seen that the fracture occurs earlier in mechanically damaged hair (10%) than in chemically damaged hair

(20%). This could be because in mechanically damaged hair parts of the cuticle have already broken away, and cuticle damage is more extensive than in chemically damaged hair.

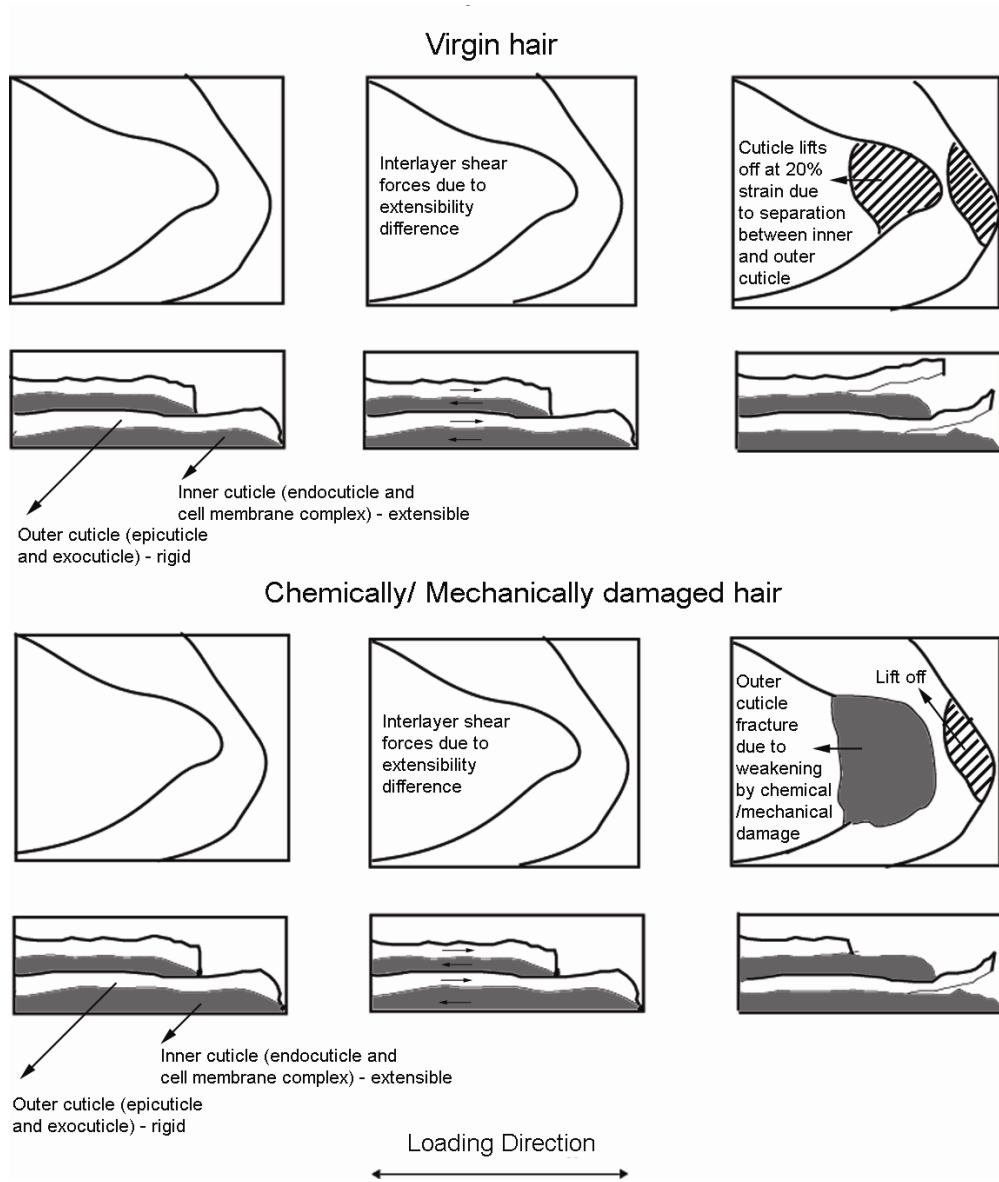


**Figure 2.5** Schematic of the progress of morphology change in virgin and damaged hair. Top and cross sectional views are shown. In the case of virgin hair, lift off of cuticle outer layer is seen. Whereas in damaged hair, both lift off and cuticle fracture is noticed.

#### **2.2.4 Effect of conditioner treatment**

Figure 2.4 (a) and 2.4 (b) also present images for virgin and chemically damaged hair treated with one cycle of conditioner. Conditioner has no apparent effect on the lift off or fracture phenomenon. Virgin treated hair continues to show only lift off and chemically damaged treated hair continues to show both lift off and fracture. Conditioner coats the cuticle and improves its tribological properties (LaTorre *et al.*, 2006, Bhushan *et al.*, 2005). However it does not chemically or physically alter the cuticle in any way. Both lift off and fracture are dependent on the mechanical properties of the cuticle, these are not changed by the conditioner. Hence, conditioner neither improves nor degrades the tensile response of human hair.

#### **2.2.5 Tensile properties and response of ethnic hair**

Figure 2.6 presents stress strain curves for the three categories of ethnic hair - Caucasian, Asian and African, and Table 2.2 displays the calculated mechanical properties. . The elastic modulus is calculated by fitting a line to the linear portion of the curve and finding its slope. The yield stress is taken as the highest point of this linear portion. The strain and stress at the point where the fiber fails are taken as the strain to break and the breaking strength respectively. All the values presented are average values based on 15 measurements.

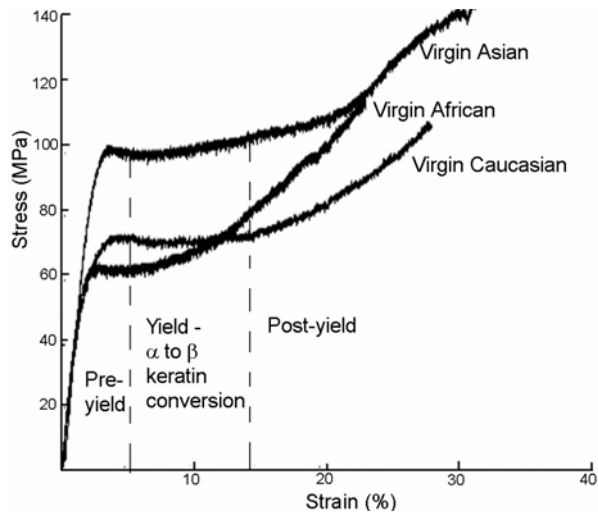


**Figure 2.6** Stress strain curves for virgin Caucasian, Asian and African hair. Transition from alpha to beta keratin is the reason for the unique shape of these curves.

From the stress strain curves, it is seen that in general, Asian hair has the highest ultimate strength and strain to break, followed by Caucasian hair. African hair shows very low mechanical properties in terms of modulus, yield point and strain to break. The lowered mechanical properties of African hair are thought to be partly arising from the higher stresses encountered by it during normal combing and detangling due to its characteristic curly structure (Kamath and Hornby, 1984). The stress strain curves presented are based on 15 individual measurements.

**Table 2.2** Mechanical properties of ethnic hair - The values presented here are based on 15 measurements. Values show upto 15% variation from sample to sample.

	Caucasian	Asian	African
Elastic modulus (GPa)	3.3	4.7	2.5
Yield strength (MPa)	67	100	58
Breaking strength (MPa)	117	139	101
Strain at break (%)	35	32	20

Figure 2.7 shows AFM topographical images, and 2-D profiles at indicated planes, of a given control area with increasing strain, of virgin Caucasian, Asian and African hair. The effect of tension on Caucasian and Asian hair is quite similar. The most significant effect of tension in both cases is lifting of the outer cuticle layer. As mentioned earlier, human hair cuticles have a lamellar structure and the various layers of human hair vary in their cystine content. This causes variation in their mechanical strength. The epicuticle and exocuticle (the outer cuticle) are high in cystine content and are extremely rigid. The endocuticle and cell membrane complex (the inner cuticle) are low in cystine content and are more extensible. Stretching hair sets up interlayer shear forces due to this difference in extensibility (Ruetsch and Weigmann, 1996; Seshadri and Bhushan, 2008). This causes the inner cuticle to fail, and the outer cuticle lifts off producing the change in height and slope of the AFM images and 2-D profiles. For virgin Caucasian hair, this inner cuticle failure and outer cuticle lift off occurs at about 20% strain, where as for Asian hair noticeable lift off occurs later at around 24% strain. Also, compared to Caucasian hair, the number of cuticle edges that lift off are fewer in Asian hair. These differences could be caused because the inner cuticle of Asian hair is also

quite rigid. This reduces the extensibility difference between the outer and inner cuticle and hence the magnitude of the interlayer shear force is reduced.

African hair cuticle shows a complete rupture at around 20% strain. This is seen as the indistinct image obtained at 20% strain. Generally, even virgin African hair cuticles are seen to have undergone considerable amount of cuticle damage due to combing and detangling. This might cause the cuticle rupture at ~20%. It is interesting to note that in line with previous observations, most failures of African hair were seen to occur in the regions of twist reversals, as stress concentrations occur in these regions (Kamath and Hornby, 1984).

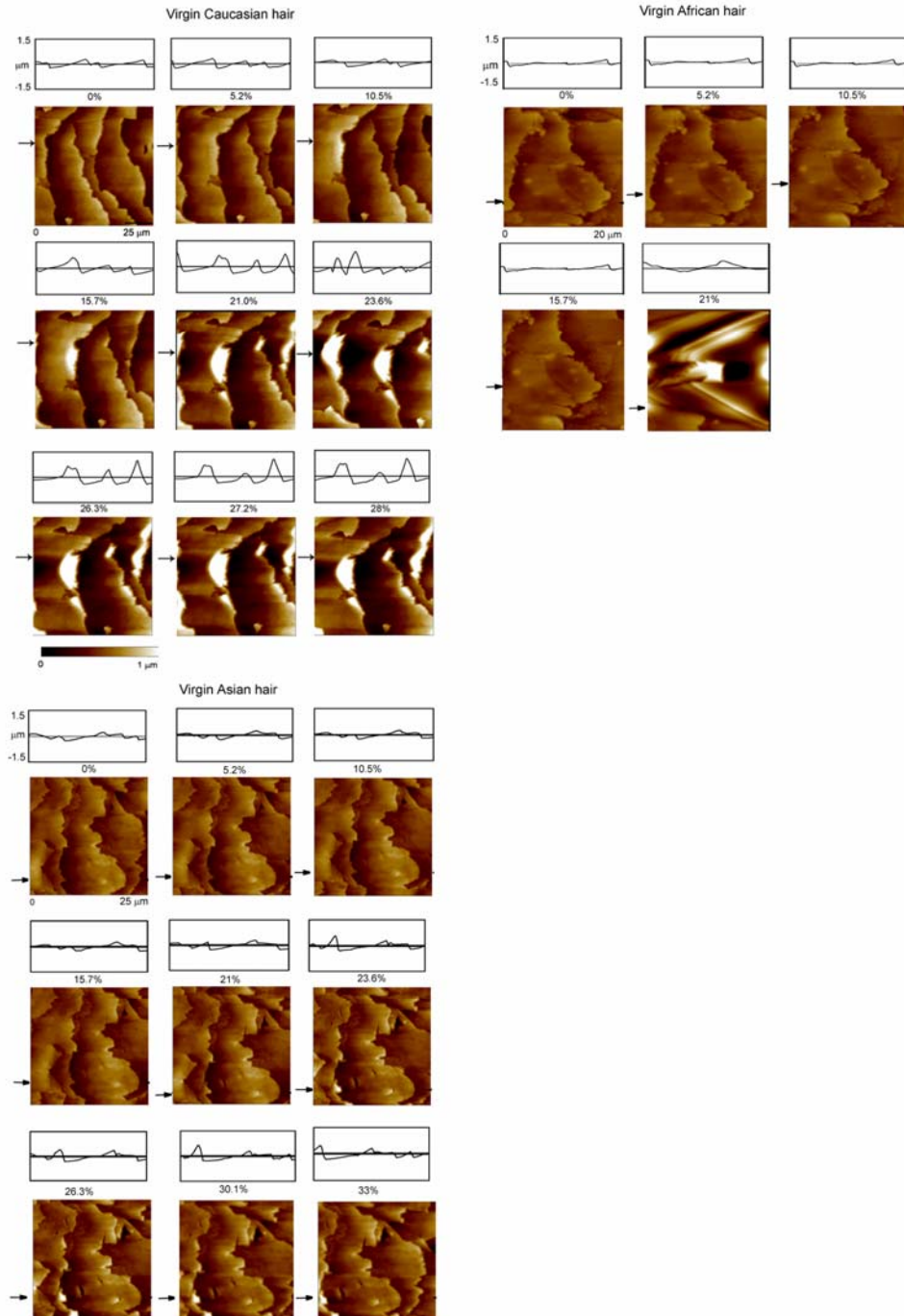


**Figure 2.7** AFM topographical images and 2-D profiles at indicated locations of a control area showing progress of damage with increasing strain in Caucasian, Asian and African hair. Caucasian hair shows cuticle lift of at ~20% and Asian at ~25%. African hair shows cuticle rupture.

## 2.2.6 Tensile properties and response of soaked hair

Wet tensile properties of human hair are generally quite different from dry tensile properties. Figure 2.8 shows stress strain curves for virgin, chemically damaged and chemically damaged treated unsoaked hair, along with curves of soaked hair of the same three types. Table 2.3 displays the calculated mechanical properties. A stress strain curve for virgin hair soaked and then dried is also presented.

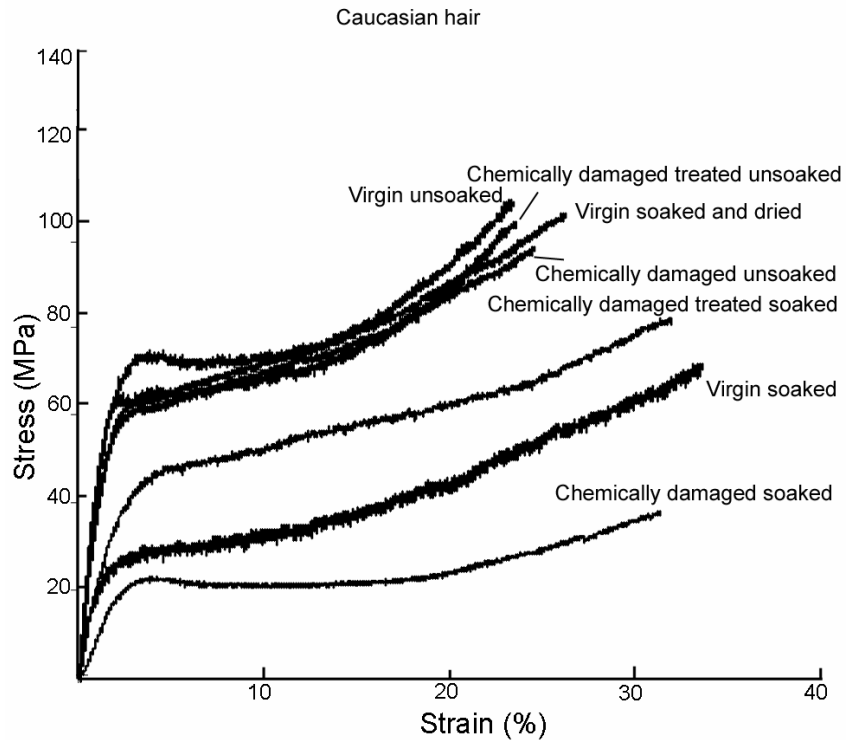


**Figure 2.8** Stress strain curves for unsoaked and soaked samples of Caucasian virgin, chemically damaged and chemically damaged treated hair and virgin soaked and dried hair.

From the stress strain curves of the unsoaked samples, it is seen that the curves almost coincide and there is no significant difference between virgin, chemically damaged and treated Caucasian hair. In the dry state, the tensile properties of hair are

significantly contributed by the cortex. Hair fibers oxidized with diperisophthalic acid, which causes almost total removal of cuticle, have shown no significant change in mechanical properties (Robbins and Crawford, 1991). In the case of chemical damage, apart from cuticle damage, oxidation of the cystine in keratin to cysteic acid residues occurs, and hence disrupts the disulfide cross links. However, the disulfide bonding does not influence tensile properties of keratin fibers in the dry state, though some effect is seen in the wet state (Robbins, 1994).

**Table 2.3** Mechanical properties of unsoaked and soaked hair. All values are based on 15 measurements. data shows a 15% variation sample to sample

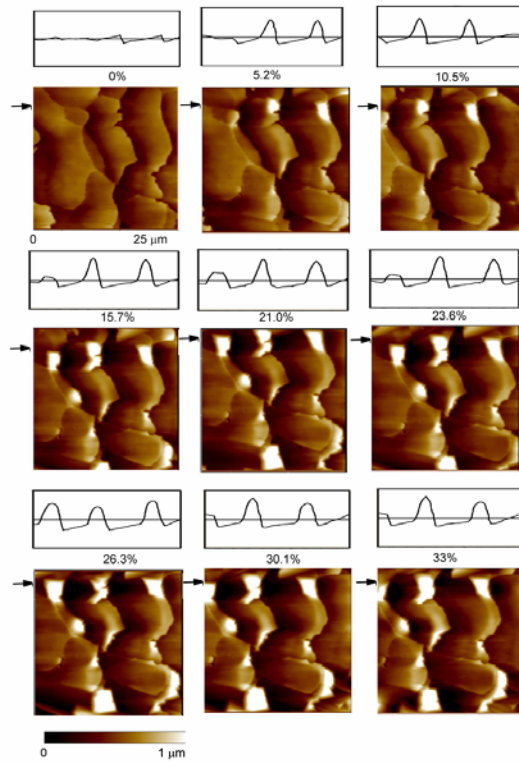
	Unsoaked			Soaked			Soaked and dried
	Virgin	Chemically damaged	Chemically damaged treated	Virgin	Chemically damaged	Chemically damaged treated	Virgin
Elastic modulus (GPa)	3.3	3.3	2.9	0.9	0.5	0.9	3.1
Yield strength (MPa)	67	61	74	28	23	47	65
Breaking strength (MPa)	117	107	108	70	37	82	106
Strain at break (%)	35	32	31	41	37	39	32

The stress strain curves of the soaked samples are considerably different from unsoaked samples. While the strain to break increases, the yield strength, ultimate strength and elastic modulus are considerably reduced by soaking. Soaking apparently softens the hair fiber. One reason for the difference in the mechanical properties is the diametrical swelling of hair in water. Human hair exhibits 14-16% diametrical swelling

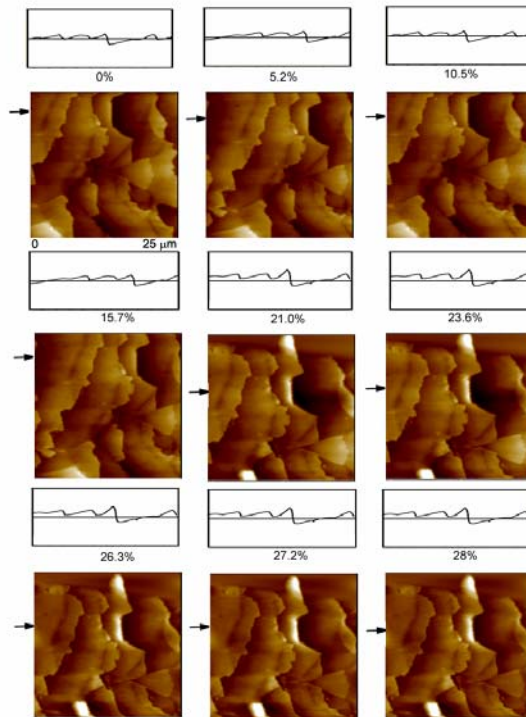
in water (Robbins, 1994). In the present experiments, the diameter of every fiber (soaked and dry) was measured prior to tension tests as described earlier. Though, a comparison between wet and dry diameter of any particular fiber was not carried out, the diameter of the wet fiber was as such used for stress computation in soaked curves, and the dry diameter for unsoaked curves. This leads to the lowered stress values on the stress strain curves. However apart from the geometric effect of the diameter, chemical changes are also thought to be responsible for this difference. It has been reported that stress strain curves of soaked and unsoaked fibers, where stress is computed using only wet diameter for both fibers still show considerable difference in mechanical properties and lowering of elastic modulus (Feughelman, 1997). Using the same diameter for both samples is justified as a form of normalization. The basis is that there is still the same amount of structural material in both soaked and unsoaked states. This finding is an indication that the elastic modulus and mechanical properties of soaked fibers, reported in this study are also contributed by chemical interactions. Feughelman (1997) postulates that, while the elastic modulus in the linear portion is mainly due to resistance of the alpha helix hydrogen bonds, Coulombic interaction bonds in the alpha helix also have a degree of contribution. In the wet state, some of the groups involved in the Coulombic bonding, interact with water instead and are broken, which leads to a lowered wet elastic modulus. The changes in mechanical properties in wet state have also been attributed to presence of high sulphur and high glycine tyrosine protein groups (Zviak, 1986). In the present study the geometric effect due to usage of different diameters for the wet and dry state, and the chemical changes in the fiber itself, may both be responsible for the differences in the mechanical properties observed in the stress strain data. Among the

soaked samples, chemically damaged hair has lowest mechanical properties, while treated hair has slightly better mechanical properties. Chemically damaged hair is more hydrophilic than virgin hair, conditioner coats the surface of damaged hair and makes the surface less hydrophilic (LaTorre *et al.*, 2006). Hence, chemical damage renders the cuticle more permeable to water leading to higher diametrical swelling. In chemically damaged treated hair, it is also possible that conditioner molecules may be occupying the path of water molecules (Wei *et al.*, 2005) leading to lesser diametrical swelling. Virgin hair which has been soaked and dried shows full recovery of mechanical properties. This again could be because the Coulombic bonding is restored when water is removed, and also the diameter decreases.

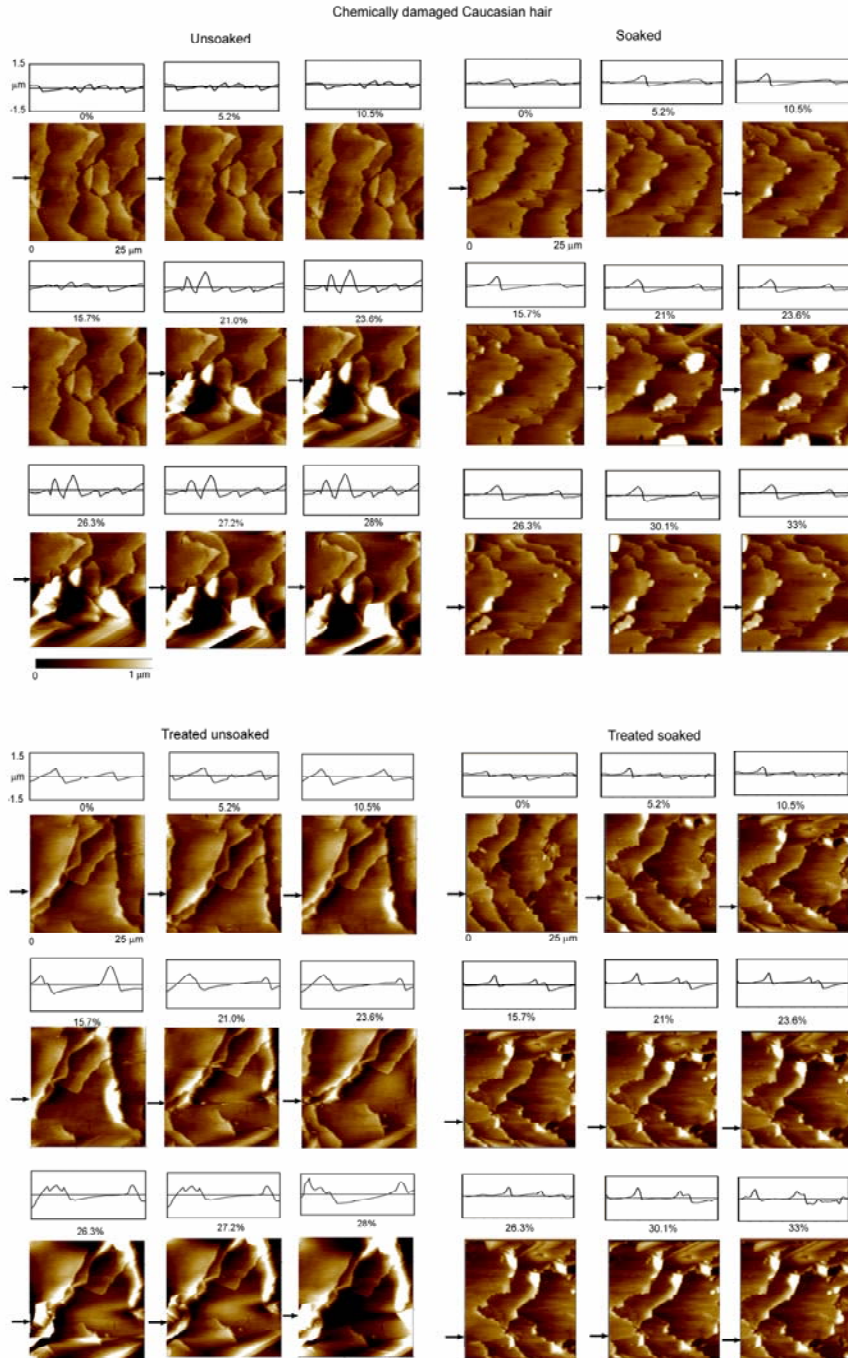
Virgin Caucasian hair  
Soaked



Soaked and dried



(a)



(b)

**Figure 2.9** AFM topographical images and 2-D profiles at indicated locations of a control area showing progress of damage with increasing strain in (a) Virgin Caucasian soaked hair and soaked and dried hair, (b) soaked and unsoaked samples of chemically damaged and chemically damaged treated hair. All soaked samples show lift off at about 5% strain. Chemically damaged and damaged treated hair show scale fracture. For treated soaked hair additional cuticles lift off at 20% strain.

Figure 2.9 (a) shows AFM images of a given control area with increasing strain for virgin soaked Caucasian hair, and virgin soaked Caucasian hair that has been dried. For the soaked sample, it is seen that cuticle lift off occurs very early, at around 5%. The reason for this is thought to be the differential penetration of water into the cuticle. Human hair shows a net swelling of 15% in diameter in water. This swelling is usually explained in terms of the microfibril and matrix components of the cortex. However, it has been proved by X-ray diffraction measurements, that only 5.5% of swelling occurs in these regions (Spei and Zahn, 1979). Later studies (Swift, 1991; Kreplak *et al.*, 2001) attribute this difference to the non keratinous proteins of the fiber, namely the endocuticle and the cell membrane complex, which are also found to exhibit a large order swelling. This swelling of the non keratin proteins is probably because of the absence of significant covalent linking and the presence of hydrophilic amino acid chain groups in the inner cuticle (Swift, 1991). The swelling has also been noticed as an increase in outer cuticle average height immediately after soaking (O'Connor *et al.*, 1995) and consequently high localized cuticle loss during wet combing as compared to dry combing (Kelly and Robinson, 1982). The outer cuticle, which is extensively cross linked, remains rigid and does not swell in water. Hence when the inner cuticle swells in water, the outer cuticle is constrained from rising up at the point of its overlap with the next outer cuticle, this leads to the development of a component of force normal to its surface (Henderson *et al.*, 1978; Swift, 1997). This force causes the swollen endocuticle to crack earlier, causing the observed early cuticle lift off. After this, virgin hair images stay the same, until fiber failure occurs at around 35% strain. No cuticle fracture/ rupture is seen. Virgin soaked

and dried hair shows behavior similar to unsoaked hair. Here, lift off occurs at 20% strain, due to extensibility difference between the outer and inner cuticle.

The top half of Fig 2.9 (b) shows images for chemically damaged unsoaked hair and chemically damaged soaked hair. For chemically damaged unsoaked hair, lift off occurs at 20% due to extensibility difference between outer and inner cuticle as explained earlier. Apart from the lift off, another noticeable effect is the disappearance of some cuticle edges and the appearance of sponge like scales instead. Sponge like scales in the cuticle have been observed earlier while isolating human hair cuticle from the hair fiber, these are thought to be remains of cuticle cells, which have split upto the endocuticle (Swift and Bews, 1974). Chemical damage causes cuticle weakening. Hence in the case of chemically damaged unsoaked hair, along with failure and delaminations in the endocuticular region at 20% strain, fracture of the outer cuticle occurs to expose the inner cuticle.

In the case of soaked hair, the early lift off due to differential aqueous penetration is seen as discussed earlier. In addition, cuticle fracture is also observed. The set of images displayed, clearly show part of the cuticle breaking away, the formation of debris and clearing away of this debris towards the end of the experiment.

The bottom half of figure 2.9(b) presents data for chemically damaged, conditioner treated unsoaked and soaked hair. Damaged treated unsoaked hair shows behavior similar to damaged hair. Lift off at 20% strain and cuticle fracture are observed. Conditioner coats hair and improves its tribological properties (Bhushan *et al.*, 2005) but does not apparently affect the lift off or fracture process of the cuticle in the dry state. For damaged treated and soaked hair, the results are quite different. It is seen that few of the

cuticles lift off at ~5% strain and additional ones at 20% strain. It is possible that conditioner blocks the pathway of water molecules to some parts of the inner cuticle (Wei *et al.*, 2005). Hence, where water reaches, swelling occurs, leading to a normal force development and consequent lift off at ~5% strain. Where water is blocked from reaching, the cuticle behaves as in dry state, and lift off occurs at ~20% strain due to extensibility difference.

Figure 2.10 shows a schematic of the effect of soaking on hair morphology of virgin, chemically damaged and chemically damaged treated Caucasian hair.

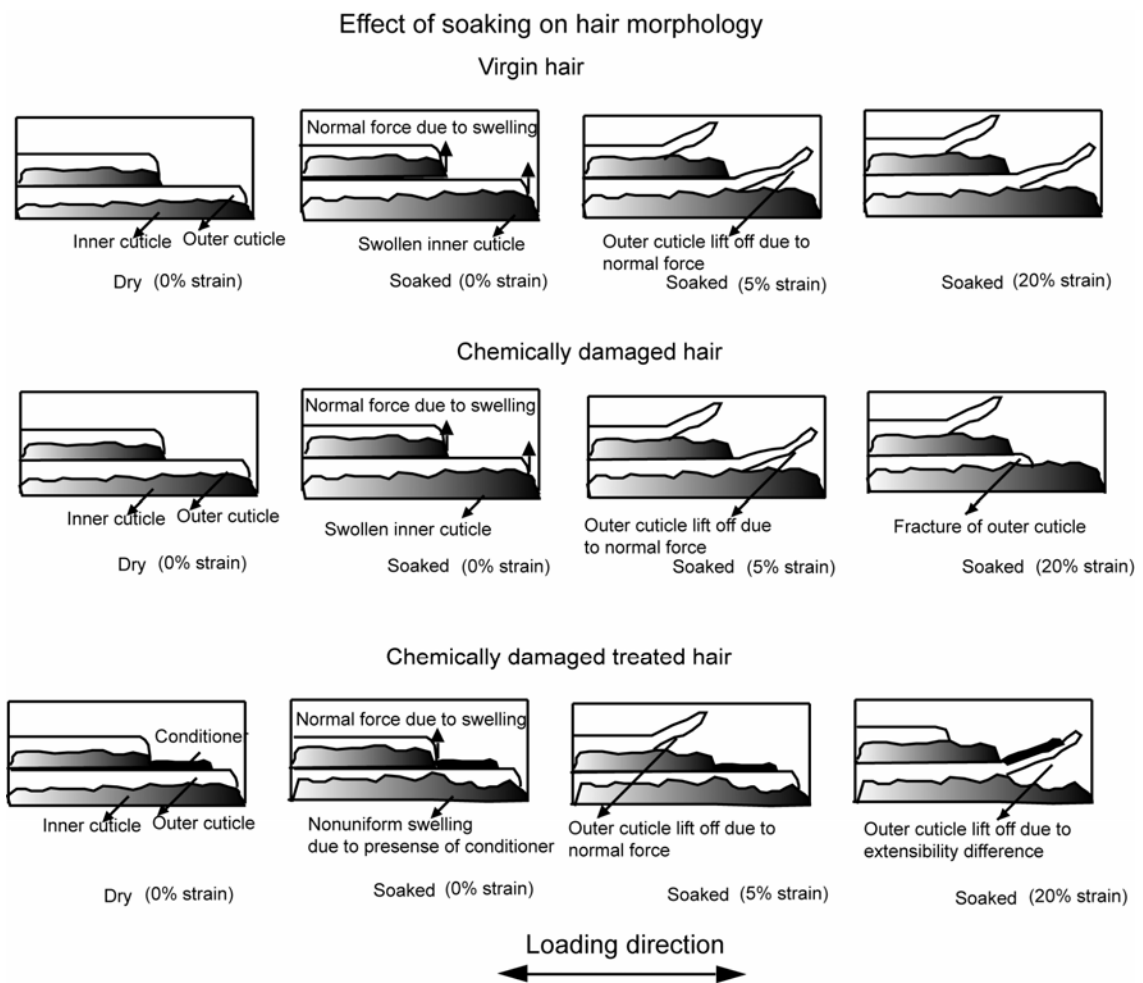


**Figure 2.10** Schematic diagram of the effect of soaking on hair morphology

### **2.2.7 Effect of fatigue on tensile properties and response**

Figure 2.11 presents stress strain curves for fatigued virgin, damaged and treated Caucasian hair fibers and Table 2.4 presents the calculated mechanical properties. It is seen that fatigue softens the hair fiber, reduces its mechanical properties and the strain to break point. A possible explanation could be that low load fatigue reduces intercellular adhesion in the cortical cells (Kamath and Hornby, 1984). This weakening of the cortex, leads to the overall reduction in mechanical properties. Again, no significant difference is seen between virgin, damaged and treated hair. The curves almost coincide. The reasons for this are most probably the same as that for unsoaked virgin, damaged and treated hair - the tensile properties in dry state are significantly determined by the cortex, and chemical damage and conditioner treatment predominantly affect the cuticle. Hence no apparent difference is seen in the stress strain curves.

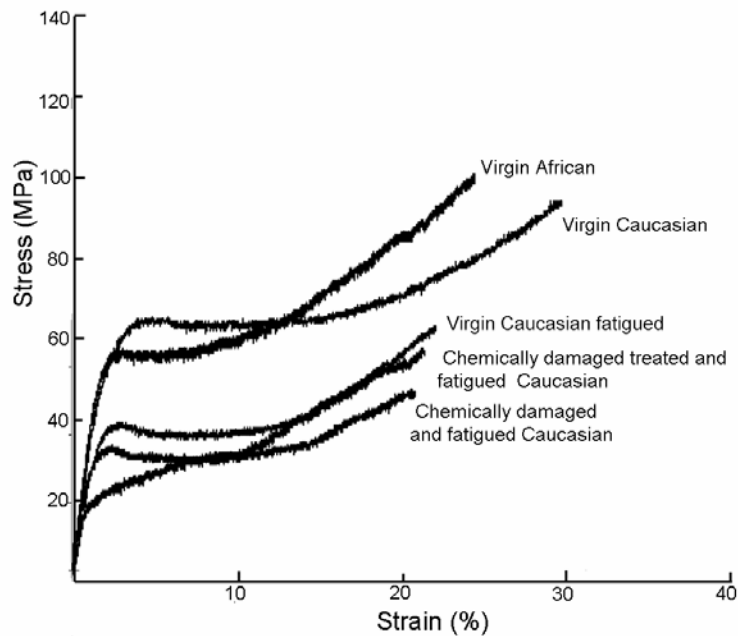


**Figure 2.11** Stress strain curves for virgin, chemically damaged and chemically damaged treated Caucasian hair subjected to fatigue. Virgin Caucasian and virgin African stress strain curves are shown for comparison

Figure 2.12 (a) shows images of virgin Caucasian hair, taken during the fatiguing process. It is seen that no visible change occurs in the surface morphology in 5000 cycles of straining, with a maximum strain of ~15%. This could be because, the first indication of failure in dry state, cuticle lift off, occurs at ~20% strain, and the maximum cyclic strain is kept below this value. Figure 2.12 (b) shows images for the tension test on virgin, damaged and treated fatigued fibers. In all three cases outer cuticle lift off occurs at 5 % strain. This is thought to be due to inner cuticle failure, caused by extensibility difference. It probably occurs earlier because the fatiguing process has already stretched it to 15% strain, and the cycling has weakened both the inner and outer cuticle. For virgin fatigued hair, in addition to lift off, cuticle fracture and appearance of spongy scales is seen, which was not seen in the dry non-fatigued tension experiments. Fatiguing hair

fibers is known to nucleate weak spots on the cuticle (Kamath and Hornby, 1984). These might propagate, on tensile load application, resulting in tearing or fracture. This is an indication of a damaged and weakened cuticle. Chemically damaged, and damaged treated hair show similar behavior. A complete rupture of the cuticle layer is noticed at 10% strain, leading to the indistinct images observed. After cuticle rupture occurs, the cortex still continues to stretch until failure at 20%. Again, as the cortex contributes mainly to the stress strain curves in dry state, this rupture of the cuticle is not observable from the stress strain curves.

**Table 2.4** Mechanical properties of fatigued hair - The values presented here are based on 5 measurements. Values show upto 15% variation from sample to sample.

	Virgin	Chemically damaged	Chemically damaged treated
Elastic modulus (GPa)	1.6	1.1	1.5
Yield strength (MPa)	36	24	42
Breaking strength (MPa)	63	52	70
Strain at break (%)	20	20	21



It is interesting to note that African hair shows very similar behavior to damaged fatigued hair. Figure 8 shows the stress strain curve of African hair along with the fatigue samples. Full cuticle rupture is seen in African hair, also it shows a strain to break point comparable to fatigued hair. The shape of the stress strain curve is also similar to fatigued hair, except that the mechanical properties are higher. These similarities could be because African hair undergoes considerable cuticle damage and fatigue due to its tendency to tangle, even during normal grooming processes. This causes it to show behavior similar to fatigued and damaged Caucasian hair. The mechanical properties of African are probably higher, because hair recovers some of its mechanical properties on relaxation. Table 2.5 presents a summary of the effect of ethnicity, soaking and fatigue on tensile properties of hair.

**Table 2.5** Summary of failure modes of various hair samples

Test matrix		Strain at break (%)	Observations
Ethnicity	Caucasian	31	Appreciable outer cuticle lift off occurs at ~20% strain due to outer cuticle failure. No cuticle rupture/fracture occurs.
	Asian	35	Appreciable outer cuticle lift off occurs at ~25% strain due to inner cuticle failure. No cuticle rupture/fracture. Lift off area is lesser than Caucasian hair.
	African	20	Lowest strain to failure. Full rupture of cuticle and fiber failure occurs at ~20% strain Failure mode is similar to fatigued and chemically damaged Caucasian hair.
Soaking (Caucasian)	Virgin	38	Cortex and inner cuticle swell appreciably and hair is softened. Outer cuticle lift off occurs at ~5% strain due to swollen inner cuticle. No cuticle rupture/fracture.
	Virgin soaked and dried	31	All properties are same as virgin Caucasian hair. Full recovery on drying.
	Chemically damaged	36	Cortex and inner cuticle swell appreciably and hair is softened. Outer cuticle lifts off at ~5% strain due to swollen endocuticle. Outer cuticle fractures at ~20% strain.
	Chemically damaged and treated	35	Non uniform swelling due to presence of conditioner. Some of the outer cuticle edges lift off at ~5% strain and additional ones at ~20% strain. Outer cuticle fractures at ~20% strain.
Fatigue (Caucasian)	Virgin	20	Weakened cuticle and fiber softening occurs. Outer cuticle fractures and fiber fails at ~20% strain. No cuticle rupture occurs.
	Chemically damaged	19	Damaged cuticle is further weakened, fiber softening. Outer cuticle ruptures and fails at ~20% strain.
	Chemically damaged and treated	20	Damaged cuticle is further weakened, fiber softens. Outer cuticle ruptures and fails at ~20% strain.

## CHAPTER 3

### NANOSCALE CHARGING CHARACTERIZATION

#### 3.1 Experimental

##### 3.1.1 Hair samples

Hair samples were received from Procter & Gamble (Cincinnati, OH) and prepared per Appendix A. Four main categories of hair samples were studied: virgin, chemically damaged, mechanically damaged and treated. Virgin samples are considered to be baseline specimens and are absent of chemical damage. Chemically damaged hair fibers have been bleached and colored, which are representative of common hair management and alteration. Mechanically damaged samples were subjected to combing and were observed under an optical microscope at 100x and found to exhibit a high degree of cuticle damage. Treated samples have been treated with one cycle of a Procter & Gamble commercial conditioner containing PDMS silicone or another Procter & Gamble commercial conditioner containing amino silicone. Unless specifically stated to be amino silicone conditioner, ‘treated’ samples are treated with PDMS silicone conditioner. PDMS silicone conditioner only physically attaches to the hair surface and remains mobile (LaTorre and Bhushan, 2006, LaTorre *et. al.*, 2006). The amino silicone

is believed to chemically attach to the hair surface creating a more uniform, complete coat of conditioner (LaTorre and Bhushan, 2006; LaTorre *et. al*, 2006). It is of interest whether or not this affects the surface charge behavior of hair. All hair samples had undergone two rinse/wash cycles of commercial shampoo treatment (in the case of treated samples, prior to conditioner treatments). The samples of interest in this portion of the thesis are Caucasian virgin, Caucasian chemically damaged, Caucasian chemically damaged PDMS treated, Caucasian chemically damaged amino silicone treated, and Caucasian mechanically damaged.

The samples arrived as hair swatches approximately 0.3 m long. Although the exact location from the root is unknown, it is estimated that hair samples used for testing were between 0.1 and 0.2 m from the scalp. The tests were conducted on the middle parts of hair samples. Hair specimens were mounted on an AFM sample puck in Liquid Paper<sup>®</sup> on insulating electrical tape.

### **3.1.2 Charging and Kelvin probe microscopy**

All experiments were performed with a MultiMode atomic force microscope equipped with a Nanoscope III controller and an Extender Electronics module (Digital Instruments, CA). The Extender allows for surface potential measurements to be taken.

A Co/Cr coated conducting Si tapping mode tip (MESP, Veeco Probes) with cantilever spring constant 2.8 N/m was used for both rubbing and surface potential measurement in this study. The charge produced while rubbing on a nanoscale with an unbiased tip, was found to be within the noise level of the KPM measurement. Hence, in

order to produce a background charge repeatably on hair surface, it was found essential to apply a small DC voltage bias of 6V to the tip, while rubbing. Previous studies have also found that a small DC bias charges polymer surfaces consistently (Saurenbach and Terris, 1992). This bias was kept constant for all hair samples in this study. So while the voltage serves to produce a measurable background contrast in potential, it cannot be responsible for the differences in surface potential change between various samples or rubbing loads.

In order to charge a control area on the hair surface, the tip with zero voltage bias was first engaged on to the surface in contact mode and scanned once over a  $40\ \mu\text{m} \times 20\ \mu\text{m}$  area, at the lowest possible load (lesser than 100nN). Next, a  $10\ \mu\text{m} \times 10\ \mu\text{m}$  control area was selected for rubbing. By adjusting the contact mode setpoint and looking at the force calibration plot, the rubbing normal load was set at the required value.

Simultaneously, the DC voltage bias of 6V was applied to the tip, internally, through the controller. The voltage biased tip was then rastered once over this  $10\ \mu\text{m} \times 10\ \mu\text{m}$  area, at the increased load. This lead to charging of the hair surface. The rubbing normal load was successively increased in steps of 100 nN, from 450 nN to 750 nN.

At each load step, before and after the rubbing process, surface potential measurements were taken in situ over the same  $40\ \mu\text{m} \times 20\ \mu\text{m}$  area. The surface potential measurements were taken using AFM based KPM. Surface potential measurement with KPM is a two pass method. In the first pass, surface topography is measured using the standard AFM tapping mode. A schematic of this operation is shown in Fig. 3.1(a). In the second pass, the tip is scanned over the previously measured topography at a specified distance above the surface. In this study that distance is 10 nm. A schematic of the second pass is shown in Fig. 3.1(b). In the second pass the piezo

normally oscillating the tip in tapping mode is turned off. Instead an oscillating voltage is applied directly to the conducting tip which generates an oscillating electrostatic force.

The oscillating force has amplitude described by the following equation:

$$F = dC/dz v_{dc} v_{ac} \quad \text{Eq(3.1)}$$

$dC/dz$  – vertical derivative of tip-sample capacitance

$v_{dc}$  – dc voltage difference between tip and sample

$v_{ac}$  – amplitude of oscillating voltage applied to tip

To measure the surface potential, a dc voltage is applied to the tip until  $v_{dc}$  is equal to zero, giving zero oscillating force amplitude. Thus the surface potential at that point will equal the dc voltage applied to the tip to give zero oscillating force amplitude. No voltage from an external source was applied to the sample or the tip during either the charge deposition or the measurement process. The bias applied to the tip was internal. Hence jumper settings on the microscope were left in the factory setting shown in Fig 3.1(c).

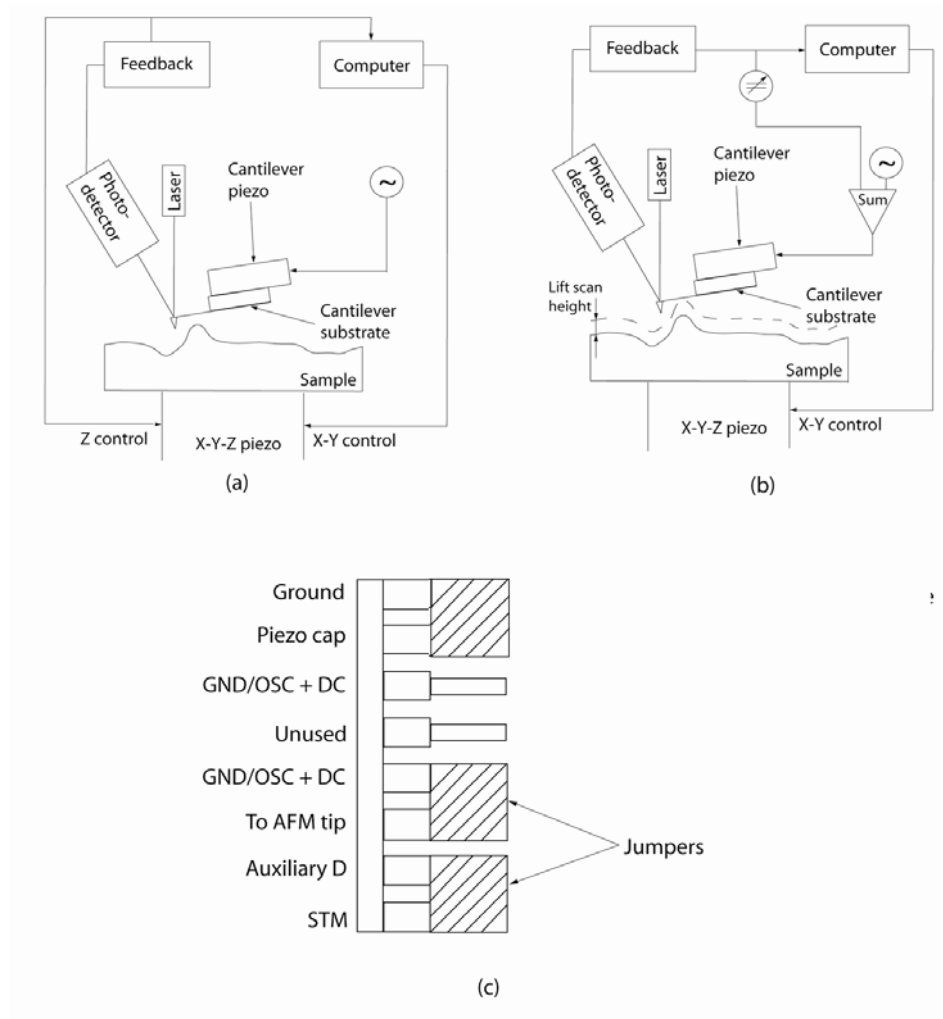


**Figure 3.1** Schematic of first pass of Kelvin probe technique measuring surface height (Bhushan and Goldade, 2000a); (b) Schematic of second pass of Kelvin probe technique measuring surface potential (Bhushan and Goldade, 2000a); (c) Jumper configuration during surface potential measurement for all data shown.

It should be noted that rubbing and surface potential measurements were done using the same tip. The condition of the tip was verified before and after a set of experiments, by putting in a known voltage to a metal sample puck, and measuring it. The measurement was found to be unaffected. Hence rubbing does not affect the ability of the tip to measure surface potential. This is probably because hair surface is soft

compared to the tip, and the rubbing loads are also kept below the level where damage to tip or hair surface occurs. All experiments were carried out at ambient conditions.

## **3.2 Results and discussions**

### **3.2.1 Charging characteristics of virgin hair**

Fig 3.2 shows the change in potential after charge deposition in virgin hair at two normal loads. All images in this section are arranged in three columns. The first column is the topography of the control area. The second column is the surface potential map of the same area before charge deposition and wear. The third column is the surface potential map of the control area after charge deposition and wear. In the surface potential maps, an average value is subtracted out to display contrast more clearly. In the surface potential maps of hair, a contrast or increase in potential around the cuticle edges is generally observed. This is thought to be an artifact of the KPM technique (Lodge and Bhushan, 2007a, b) and hence will not be discussed further. By comparing the before and after rubbing surface potential maps in Fig 3.2 , it is seen that a marked increase in surface potential occurs over the marked area, where the surface was rubbed with a voltage biased tip, even at the lowest load.

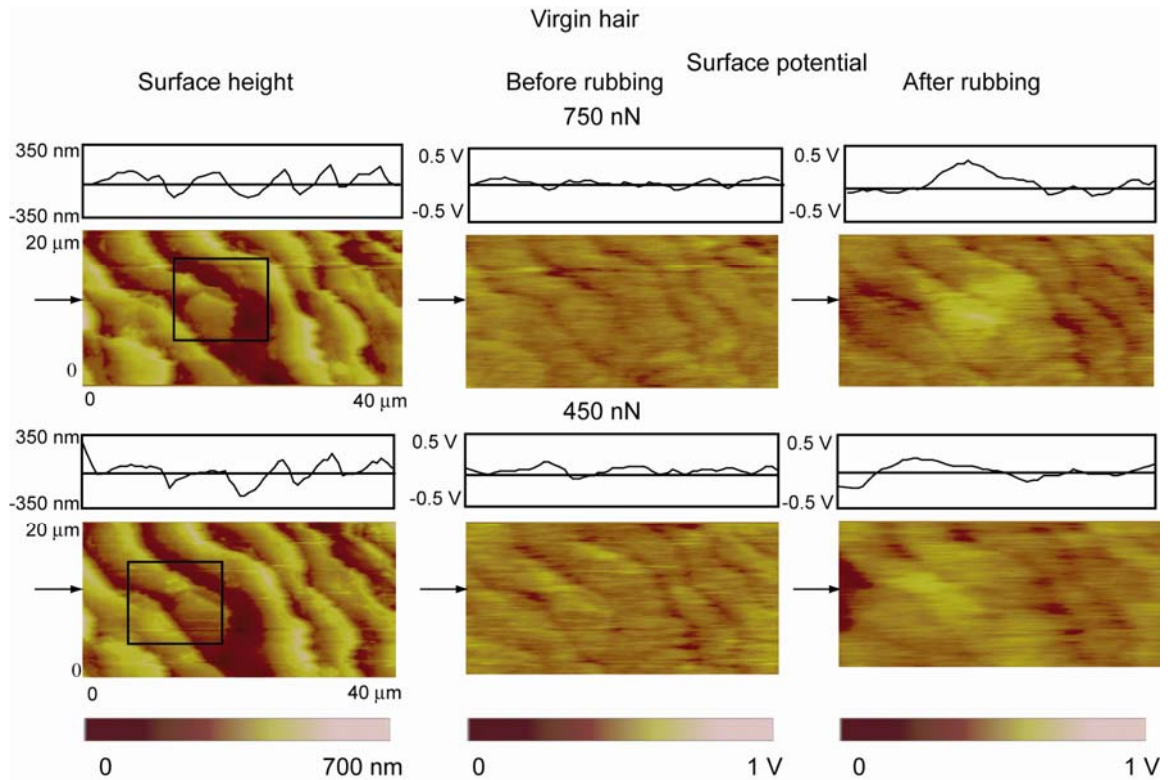


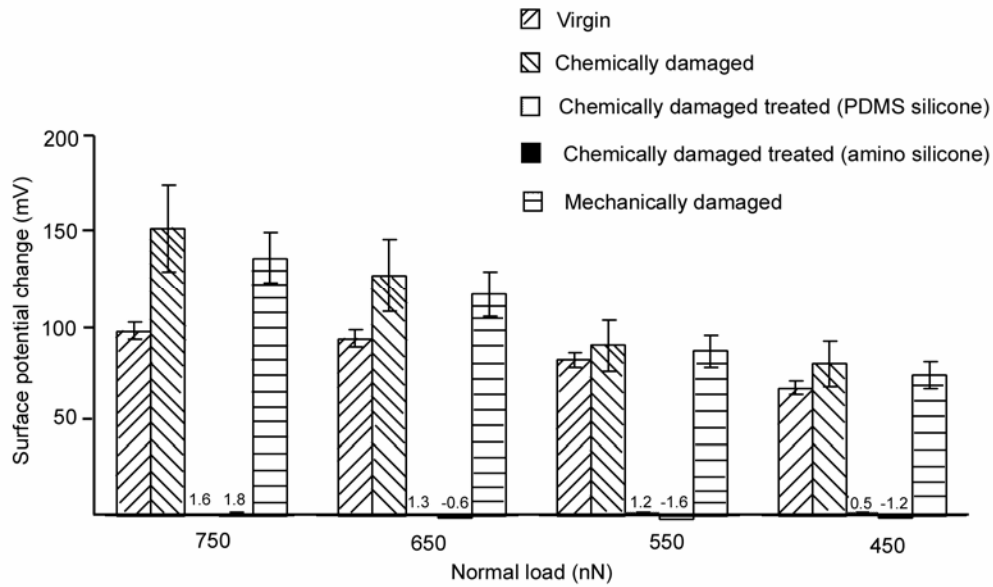
**Figure 3.2** AFM topography images and KPM surface potential maps of virgin hair before and after rubbing with voltage biased tip at two different normal loads. The area where wear and charge deposition was performed is marked on the topography image.

The tendency of hair to get charged while rubbing is partially due to its electret properties. Electrets are materials capable of storing charge and polarization. This makes them susceptible to get charged, and retain that charge during rubbing and triboelectric contact. Human hair is a natural bio-electret, and similar to other polymer electrets, displays piezoelectric and pyroelectric properties (Mascarenhas, 1980; Jachowicz, *et. al.*, 1984; Fukada, 1992; Feughelman, 2003). The natural electret properties of hair are thought to arise from the polarity of the peptide bond in the keratin molecules, and also from their synergistic arrangement in the alpha helix structuring of the cortical cells, that adds up individual molecule polarities (Mascarenhas, 1980). Electret properties have also

been observed in other biological materials like skin, bone, horn and quill. For example, electret properties of rat skin have been investigated by charging it with high voltage, and then observing thermally stimulated discharge (TSD) peaks (Lili *et. al.*, 1999). Surface charging of electrets have been studied by different methods which include contacting with a point electrode like an AFM tip to which high magnitude voltage pulses are applied (Stern *et.al.*, 1988 ) or by a pure triboelectric contact (Terris *et.al.*, 1989). Where high voltages or voltage pulses are involved, the mechanism of charge deposition is thought to be corona discharge between a point electrode (which could be an AFM tip) and the surface. Where no external voltage is applied, the mechanism is thought to be triboelectric and charge transfer takes place due to work function differences. In the present study, the actual mechanism by which the hair surface gets charged is not very clearly understood. It is thought to be a combined effect of electrostatic and triboelectric interactions between the tip and the surface. The applied voltage bias is however kept constant throughout this study, during experiments on various hair samples. The differences in measured charge hence, depends primarily on the nature of the hair surface and the rubbing process parameters, of which only rubbing load is varied in this study.

Fig 3.2 also shows surface potential images at two loads, and Fig 3.3 displays a quantitative bar chart of the change in surface potential at four different rubbing normal loads. The values displayed in the bar chart are averages over the whole charged/worn area, for measurements on at least five different samples of each type of hair tested, at each load step. For virgin hair, compared to other hair samples on the bar chart, it is seen that the surface potential change does not change much with increasing rubbing load. According to previous studies the friction force in virgin hair shows very little increase

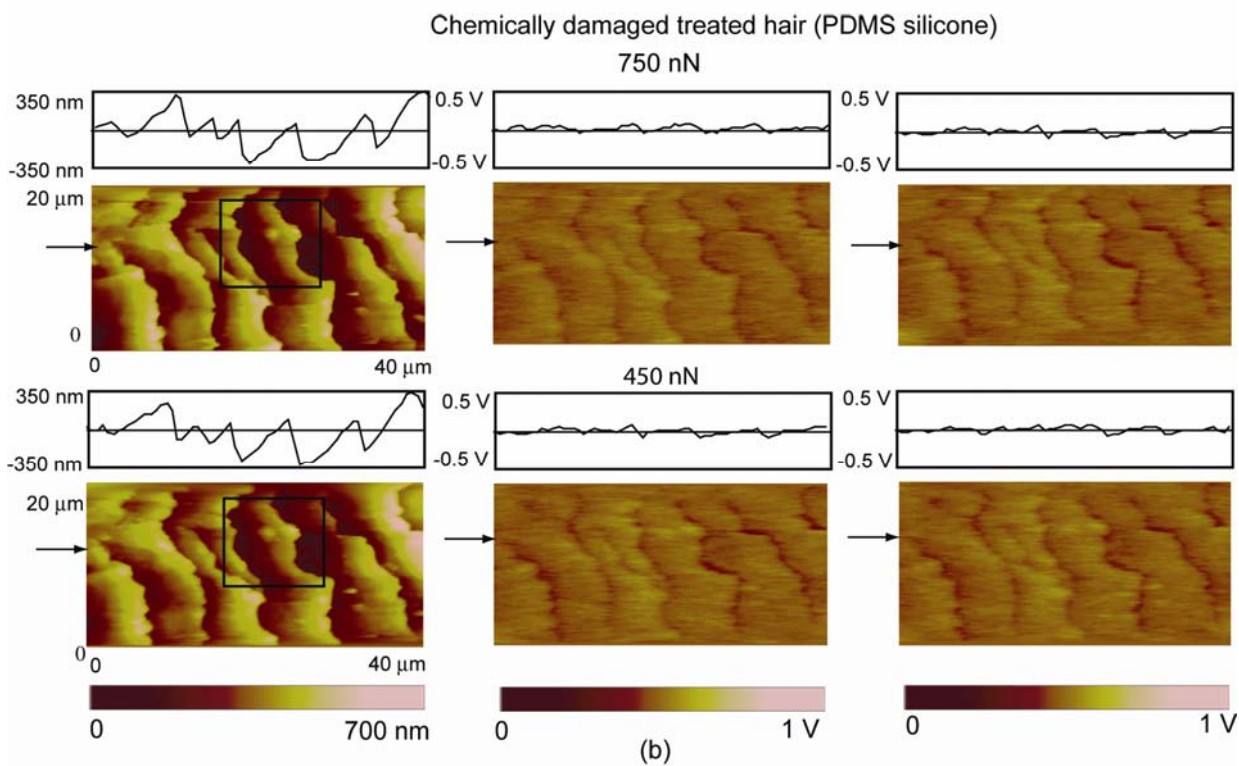
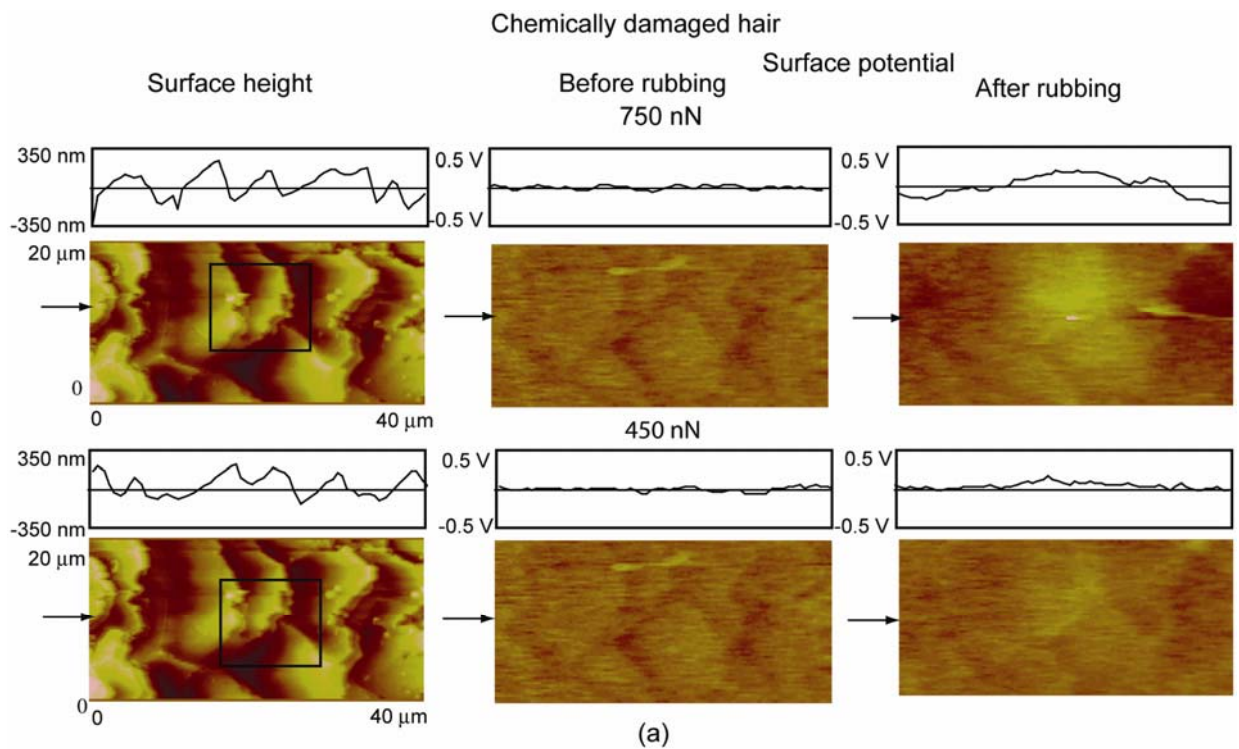
with normal rubbing load, compared to damaged hair. This is attributed to the intact lipid or 18 MEA layer on virgin hair (LaTorre and Bhushan, 2005). This layer contributes significantly to the lubricity of hair surface. Charge developed is known to increase with increasing friction between hair and rubbing element (Lunn and Evans, 1977). As the friction does not increase much with normal load, the surface potential or the charge developed also remains more or less constant.



**Figure 3.3** Bar chart showing average surface potential change and its dependence on normal load for all the hair samples studied.

### 3.2.2 Effect of damage on charging characteristics

Figure 3.4 (a) shows topography and surface potential maps of chemically damaged hair, before and after rubbing. Figure 3.3 displays the corresponding quantitative values at four different loads.



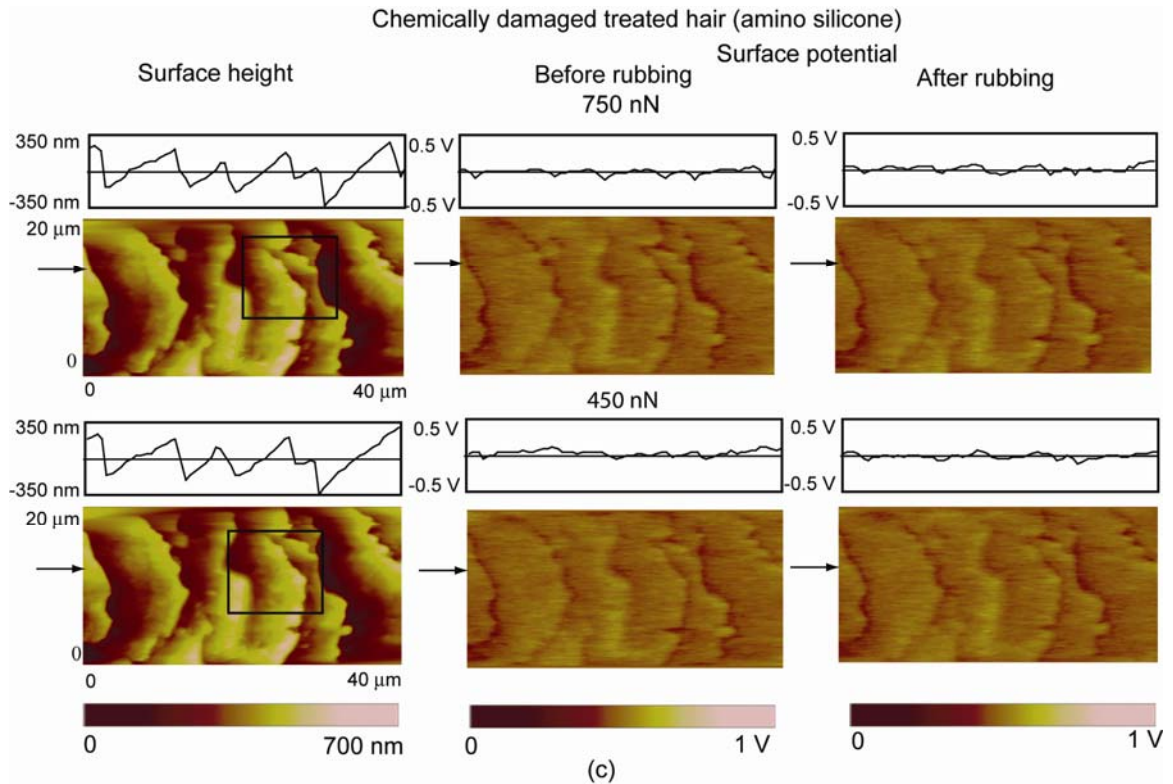


**Figure 3.4** Topography images and surface potential maps before and after rubbing with voltage biased tip at two different normal loads for (a) chemically damaged hair; (b) chemically damaged hair treated with PDMS silicone conditioner; (c) chemically damaged hair treated with amino silicone conditioner. The area where wear and charge deposition was performed is marked on the topography image.

It is observed that, at lower loads the surface potential change in chemically damaged hair is comparable to virgin hair, while at higher loads it is much more than virgin hair. In chemically damaged hair, the naturally present lipid layer is stripped away by the bleach and coloring agents (LaTorre and Bhushan, 2006, LaTorre *et. al.*, 2006). This means that there is higher friction between the tip and the surface. Also previous studies indicate that, friction increases much more rapidly with normal load in damaged hair, as compared to virgin hair (LaTorre and Bhushan, 2005). This leads to more charge generation and the increase in the surface potential change at higher loads.

Fig 3.5 displays the topography and potential maps for mechanically damaged hair; Fig 3.3 shows the quantitative values. Mechanically damaged hair shows surface potential values that are in between virgin hair and chemically damaged hair. The stripping of the lipid layer is complete in chemically damaged hair, because of the uniform nature of chemical damage. However, with mechanically damaged hair, it might be possible that the lipid layer is only partially stripped off, wherever the comb has rubbed into the fiber. Hence, the friction, and its variation with normal load is probably not as much as chemically damaged hair. However, it is still found to be higher than virgin hair.

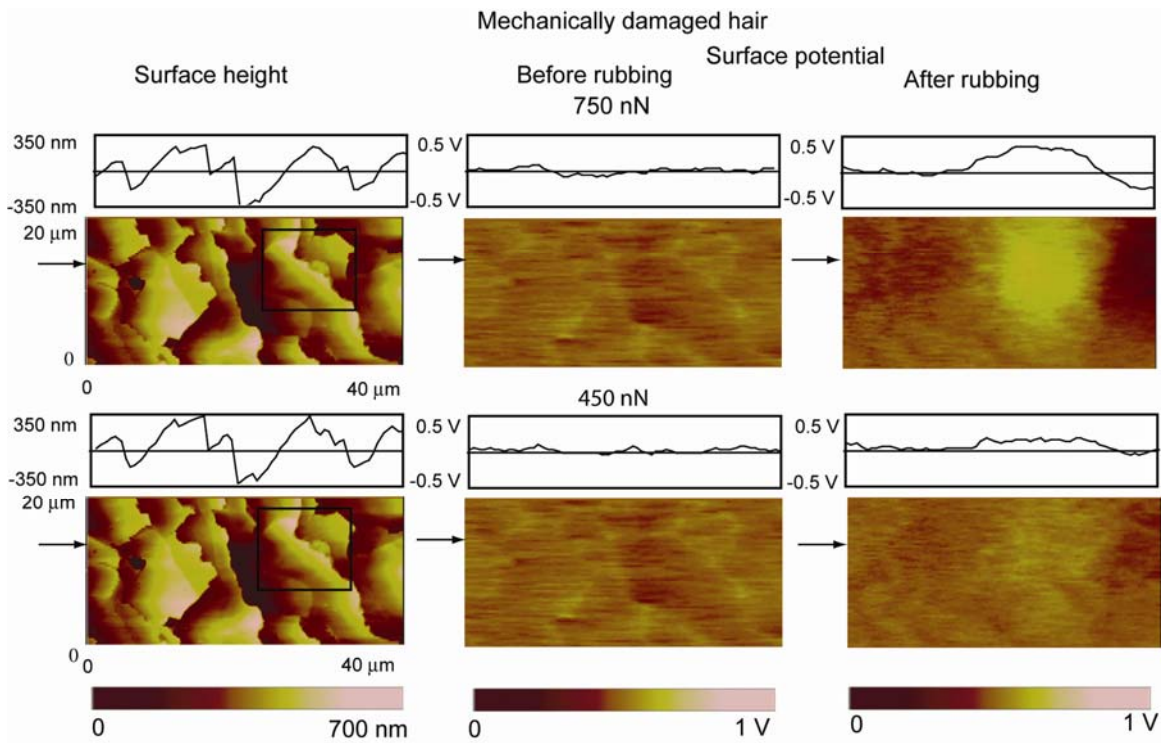


**Figure 3.5** Topography images and surface potential maps before and after rubbing with voltage biased tip for mechanically damaged hair. The area where wear and charge deposition was performed is marked on the topography image.

### 3.2.3 Effect of conditioner treatment

Figure 3.4 (b) and 3.4 (c) show surface potential maps for chemically damaged conditioner treated hair samples. Two types of conditioners were studied - PDMS silicone based conditioner, and a newer amino silicone based conditioner. Figure 3.3 again displays quantitative values of surface potential change.

It is clearly seen that both conditioners dramatically reduce the surface potential change, and charge deposition on the hair. There is almost no surface potential change due to rubbing on conditioner treated hair. Conditioners are known to possess strong antistatic properties. There are two possible mechanisms by which conditioners could reduce charge on hair (Lunn and Evans, 1977). The first is the lubricating effect of the conditioners. Conditioners are basically silicone oils that lubricate hair surface. They replenish the 18 MEA layer stripped by damage. This lower friction leads to the lower charging. However, the second and probably more dominant effect is the increase in surface conductivity. Hersh *et. al.* (1981) have reported that conditioners increase the conductivity of hair fibers. The resistance per unit length of hair decreased from  $10^{18}$  ohm/cm to  $10^{17}$  ohm/cm on conditioner treatment. So, whatever charge is deposited is quickly dissipated by the conducting conditioner layer.

Both amino silicone and PDMS silicone treated hair samples, show comparable surface potential changes. PDMS silicone physically attaches to the surface while amino silicone is chemically bonded, and hence more uniformly covers the surface. However not much difference is seen between the two conditioner's antistatic effects. This could be because surface conductivity is probably the dominant antistatic mechanism. Even a

non uniform conditioner layer significantly increases the conductivity. Also, rubbing with the AFM tip may actually be redistributing the PDMS conditioner more uniformly over the surface, especially at higher loads. Still, both the amino silicone and PDMS silicone conditioners show a significant reduction of potential compared to damaged or even virgin hair.

## CHAPTER 4

### CONCLUSIONS

In this thesis the mechanical and electrical of human hair fibers were studied in detail. A new technique that makes it possible to perform tensile experiments in-situ with an AFM was developed. This technique was employed in characterizing the tensile response of virgin, damaged, conditioner treated, ethnic, soaked and fatigued hair samples. This study has advanced previous literature in this area and is also the first attempt to study tensile properties of hair in-situ with high resolution atomic force microscopy. The understanding provided by this study, will be helpful to develop better hair care products that target specific causes of damage. Also, the current understanding of human hair, a complex biomaterial has been advanced. The second portion of this thesis looked at a common phenomenon, the static charging of hair. The static charging of hair was studied at the nanoscale employing AFM and KPM. Through this study, a systematic understanding of the charging mechanism of hair and its dependence on the rubbing process parameters was developed. Also the effectiveness of conditioners in dissipating static charge was ascertained. A summary of main conclusions from this study are as follows:

#### **4.1 In-situ tensile deformation characterization**

1. In situ tensile experiments on a single fiber of human hair with AFM facilitates systematically following the progress of deformation and morphology change by marking and imaging a fixed control area.

2. Human hair shows a stress strain curve typical of keratinous fibers. Chemical damage, mechanical damage and conditioner treatment have no obvious effect on the dry stress strain curve or tensile properties. This is because such treatments affect the cuticle predominantly and tensile properties of human hair in dry state are governed by the cortex.
3. Tensile stress in general causes lift off of the outer cuticle. The lift off is sudden and occurs consistently at around 20% strain. This lift off occurs in all types of hair studied, and is due to interlayer shear forces and consequent separation between inner and outer cuticle layers at 20% strain.
4. Chemical damage and mechanical damage cause weakening of the outer cuticle. Along with lift off, fracture of the outer cuticle to expose endocuticular layers occurs. Fracture occurs sooner (about 10% strain) in mechanically damaged hair than chemically damaged hair (about 20% strain).
5. Conditioner has no observable effect on the dry tensile response. This is because conditioner coats the cuticle and improves its tribological properties, but does not physically or chemically alter it.
6. Different ethnic hair types show considerably different mechanical properties. Caucasian hair shows outer cuticle lift off at ~20% and Asian hair at ~25% strain. This lift off is caused by extensibility differences and consequent interlayer shear forces in the cuticle. The lift off area in Asian hair is lesser. This could be because Asian hair has in general better mechanical properties than Caucasian hair. African hair shows full cuticle rupture and fiber failure at ~20% strain and

behavior similar to damaged, fatigued Caucasian hair. This is probably because of the high stresses experienced by it during normal grooming processes.

7. Soaked virgin Caucasian hair shows outer cuticle lift off at ~5% strain due to differential water penetration in the cuticle and consequent development of normal forces. Soaked chemically damaged Caucasian hair shows cuticle fracture at ~20% strain in addition to the lift off at ~5% strain. For soaked damaged treated hair, some cuticle edges lift off at ~5% strain and additional ones at ~20% strain. This could be because, water does not penetrate into the inner cuticle in the regions where conditioner is present, and lift off occurs at ~20% strain in those regions and at ~5% strain for the others.
8. Fatigue weakens the cuticle and the cortex. Virgin fatigued Caucasian hair, shows outer cuticle lift off at ~5% strain and also scale fracture. This is due to cuticle weakening and damage. Chemically damaged and chemically damaged treated fatigued Caucasian hair show a full cuticle rupture at ~15% strain in addition to lift off at 5% strain. These are again indications of cuticle weakening.

#### **4.2 Nanoscale charging characterization**

1. Rubbing with a voltage biased AFM tip is an effective way to study charging characteristics of human hair on a nanoscale in a controlled and systematic way.
2. Virgin hair shows a marked potential difference in the control area on rubbing. However, the potential difference remains almost constant with increasing

rubbing loads. This is because friction increases very gradually with normal load in virgin hair, due to an intact lubricating lipid layer.

3. Chemically damaged hair shows a higher potential change than virgin hair and also greater surface potential change with increasing normal loads. This is because friction rapidly increases with normal load, due to stripping away of the lubricating lipid layer. Mechanically damaged hair shows a potential change between chemically damaged and virgin hair, because the lubricating lipid layer is only partially stripped away
4. Both PDMS silicone and amino silicone conditioners significantly reduce potential change. This is because they increase the surface conductivity and lubricity drastically. Both conditioners are seen to show similar behavior because conductivity increase might be the most dominant mechanism. Also, the rubbing process may be redistributing PDMS silicone conditioner, so that it is as uniform as the amino silicone conditioner.

## LIST OF REFERENCES

- R. L. C. Akkermans and P. B. Warren, "Multiscale modeling of human hair," *Phil. Trans. R. Soc. Lond. A* **362**, 1783-1793 (2004)
- R.G. Barber and A.M Posner, "A method for studying the static electricity produced on hair by combing" *J. Soc. Cosmet. Chem.*, **10**, 236-246 (1958).
- B. Bhushan and A. Goldade, "Kelvin probe microscopy measurements of surface potential change under wear at low loads" *Wear*, **244**, 104-117 (2000a).
- B. Bhushan and A. Goldade, "Measurements and analysis of surface potential change during wear of single-crystal silicon (100) at ultralow loads using Kelvin probe microscopy" *Appl. Surf. Sci.*, **157**, 373-381 (2000b).
- B. Bhushan and C. LaTorre "Structural, nanomechanical and nanotribological characterization of human hair using atomic force microscopy and nanoindentation," in *Nanotribology and Nanomechanics - An Introduction, second ed.* (B. Bhushan, ed.), Springer, Berlin, Heidelberg, 2008.
- B. Bhushan, *Introduction to Tribology*, Wiley, New York, 2002
- B. Bhushan, G. Wei, and P. Haddad, "Friction and Wear Studies of Human Hair and Skin," *Wear* **259**, 1012-1021 (2005)
- B. Bhushan, C. LaTorre, G. Wei and N. Chen, "Structural, nanomechanical and nanotribological characterization of human hair using atomic force microscopy and nanoindentation," in *Springer Handbook of Nanotechnology, second ed.* (B. Bhushan, ed.), Springer, Berlin, Heidelberg 2007
- M. S. Bobji and B. Bhushan, "In situ microscopic surface characterization studies of polymeric thin films during tensile deformation using atomic force microscopy," *J. Mater. Res.* **16**, 844-855 (2001a)
- M. S. Bobji and B. Bhushan, "Atomic force microscopy study of the microcracking of magnetic thin films under tension," *Scripta Mater.* **44**, 37-42 (2001b)
- S. Breakspeak and J. R. Smith, "Returning to the same area of hair surfaces before and after treatment: a longitudinal AFM technique," *J. Microscopy* **215**, 34-39 (2004)

- N. H. Chen and B. Bhushan, "Morphological, nanomechanical and cellular structural characterization of human hair and conditioner distribution using torsional resonance mode with an AFM," *J. Microscopy* **220**, 96-112 (2005)
- S. Dekoi and J. Jedoi, "Hair low-sulphur protein composition does not differ electrophoretically among different races," *J. Dermatol.* **15** 393-396 (1988)
- S. Dekoi and J. Jedoi, "Amount of fibrous and matrix substances from hair of different races," *J. Dermatol.* **19** 62-64 (1990)
- D. DeVecchio and B. Bhushan, "Use of a nanoscale Kelvin probe for detecting wear precursors" *Rev. Sci. Instrum.*, **69**, 3618-3624 (1998).
- A. Feughelman, *Mechanical Properties and Structure of Alpha-Keratin Fibres: Wool, Human Hair and Related Fibres*, University of South Wales Press, Sydney (1997)
- J. Gray, "Hair Care and Hair Care Products," *Clinics in Dermatology* **19** 227-236 (2001)
- P. L. Grady and S. P. Hersh, "The effect of internal additives on the electrical conductivity and activation energy of nylon fibers", *IEEE Trans. Indus. Appl.* **1A-13**, 379-385 (1977).
- G. H. Henderson, G. M. Karg, J.J. O'Neill, "Fractography of human hair," *J. Soc. Cosmet. Chem.* **29**, 449-467 (1978)
- S. P. Hersh, P. L. Grady and G. R. Bhat, "Effect of internal and external tensides on the electrical properties of polymeric surface" *Pure and Appl. Chem.* **53**, 2123-2134 (1981).
- A. Feughelman, D. Lymanb, E. Menefee , B. Willis, "The orientation of the  $\alpha$ -helices in  $\alpha$ -keratin fibres ," *Intl. J. of Biol. Macromol.* **33**, 149-152 (2003).
- E. Fukada, "Bio-electrets and Bio-piezoelectricity," *IEEE Trans. On Elec. Insul.* **27** 813-819 (1992).
- J. Jachowicz, G. Wis-Surel and L.J. Wolfram, "Directional triboelectric effect in keratin fibers," *Text. Res. J.* **54** 492-495 (1984).
- J. Jachowicz, G. Wis-Surel, M.L. Garcia, "Relationship between triboelectric charging and surface modifications of human hair" *J. Soc. Cosmet. Chem.*, **36**, 189-212 (1985).
- Y. K. Kamath and S. B. Hornby, "Mechanical and fractographic behavior of Negroid hair," *J. Soc. Cosmet. Chem.* **35**, 21-43 (1984)

- Y. K. Kamath, C.J. Dansizer, H.D. Weigman, "Wetting behavior of human hair fibers." *J. Appl. Poly. Sci.* **22**, 2295-2306 (1978).
- S. E. Kelly and V. N. E. Robinson, "The effect of grooming on the hair cuticle," *J. Soc. Cosmet. Chem.* **33**, 203-215 (1982)
- L. Kreplak, C. Merigoux, F. Briki, D. Flot and J. Doucet, "Investigation of human hair cuticle structure by microdiffraction - direct observation of cell membrane complex swelling," *Biochimica et Biophysica Acta* **1547**, 268-274 (2001)
- L. Kreplak, A. Franbourg, F. Briki, F. Leroy, J. Doucet, "A new deformation model of hard  $\alpha$ -Keratin fibers at the nanometer scale: Implications for hard  $\alpha$ -Keratin intermediate filament mechanical properties, *Biophysical J.* **82**, 2265-2274 (2002)
- C. LaTorre and B. Bhushan, "Nanotribological characterization of human hair and skin using atomic force microscopy," *Ultramicroscopy* **105**, 155-175 (2005a)
- C. LaTorre and B. Bhushan, "Nanotribological effects of hair care products and environment on human hair using atomic force microscopy," *J. Vac. Sci. Technol. A* **23**, 1034-1045 (2005b)
- C. LaTorre , B. Bhushan, J.Z. Yang, P.M. Torgerson, "Nanotribological effects of silicone type and deposition level and surfactant type on human hair using atomic force microscopy," *J. Cosmetic Sci.* **57**, 37-56 (2006)
- B. Lindelof, B. Forslind, M. S. Hedblad, "Human hair form. Morphology revealed by light and scanning electron microscopy and computer aided three-dimensional reconstruction," *Arch. Dermatol.* **124** 1359-1363 (1988)
- J. Menkart, L. J. Wolfram, and I. Mao, "Caucasian hair, Negro hair, and wool: similarities and differences," *J. Soc. Cosmet. Chem.* **35** 21-43 (1984)
- S. D. O'Connor, K. L. Komisarek and J. D. Baldeschwieler, "Atomic force microscopic study on environmental effects on hair morphology," *J. Invest. Dermatol.* **105**, 96-99 (1995)
- R. A. Lodge and B. Bhushan, "Surface characterization of human hair using tapping mode atomic force microscopy and measurement of conditioner thickness distribution", *J. Vac. Sci. Tech. A*, **24**, 1258-1269 (2006a).
- R.A. Lodge and B. Bhushan, "Wetting properties of human hair by means of dynamic contact angle measurement" *J. App. Poly. Sci.* **102**, 5255-5265 (2006b).
- R.A. Lodge and B. Bhushan, "Surface potential measurement of human hair using Kelvin probe microscopy" *J. Vac. Sci. Tech. A*, **25** 893-904 (2007a).

- R. A. Lodge, B. Bhushan, "Effect of wear and triboelectric contact on surface charge as measured by Kelvin probe microscopy," *J. Colloid Interf. Sci.* **310** 321-330 (2007b).
- C. Lili, J. Jian, X. Zhongfu and S. Chengrong, "The study of electret behavior of rat skin with thermally stimulated discharge(TSD)," *10<sup>th</sup> Intl. Symp. On Electrets* IEEE, New York (1999).
- A.C. Lunn and R.E. Evans, "The electrostatic properties of human hair" *J. Soc. Cosmet. Chem.*, **28**, 549-569 (1977).
- S. Mascarenhas, "Bioelectrets: Electrets in biomaterials and biopolymers", in *Electrets*, G. M. Sessler (ed. ), *Topics in Applied Physics* **33**, Springer-Verlag, Heidelberg, 1980.
- C.M. Mills, V.C. Ester, H. Henkin, "Measurement of static charge on hair", *J. Soc. Cosmet. Chem.*, **7**, 466-475 (1956).
- K. Morioka, *Hair Follicle – Differentiation Under the Electron Microscope*, Springer-Verlag, Tokyo, 2005.
- A.P. Negri, H.J. Cornell, "A Model for the Surface of Keratin Fibers." *Textile Res. J.* **63**, 109-115 (1993).
- C. Robbins and R. J. Crawford, "Cuticle damage and the tensile properties of human hair," *J. Soc. Cosmet. Chem.* **42**, 59-67 (1991)
- C. Robbins, *Chemical and Physical Behavior of Human Hair*, 3<sup>rd</sup> Edition, Springer-Verlag, New York, 1994
- C. R. Robbins and R. J. Crawford, "Cuticle damage and the tensile properties of human hair," *J. Soc. Cosmet. Chem.* **42**, 59-67 (1991)
- N. S. Tambe, B. Bhushan, "In situ study of nano-cracking in multilayered magnetic tapes under monotonic and fatigue loading using an AFM," *Ultramicroscopy* **100**, 359-373 (2004)
- S. B. Reutsch and H. G. Weigmann, "Mechanism of tensile stress release in the keratin fiber," *J. Soc. Cosmet. Chem.* **47**, 13-26 (1996)
- I. P. Seshadri and B. Bhushan, "In-situ tensile deformation characterization of human hair with atomic force microscopy", *Acta Mater.* **56**, 774-781 (2008).
- M. Spei and H. Zahn,"X-Ray small angle examination of swollen keratin fibers," *Melliand Textilberichte* **60**, 523-525 (1979)
- J. A. Swift, "The mechanics of fracture of human hair," *Int. J. Cosmet. Sci.* **21**, 227-239 (1999)

- J. A. Swift and B. Bews, "The chemistry of human hair cuticle-I: A new method for the physical isolation of the cuticle," *J. Soc. Cosmet. Chem.* **25**, 13-22 (1974)
- J. R. Smith and J.A. Swift, "Lamellar subcomponents of the cuticular cell membrane of mammalian keratin fibers show friction and hardness contrast by AFM," *J. Microscopy* **206**, 182-193 (2002)
- J. A. Swift, "Morphology and histochemistry of human hair", in *Formation and Structure of Human Hair* ( P. Jolles, H. Jahn, H. Höcker, eds. ) Birkhäuser, Basel (1997)
- J. A. Swift, "The mechanics of fracture of human hair," *Int. J. Cosmet. Sci.* **21**, 227-239 (1999)
- J. A. Swift, S. P. Chahai, N. J. Challoner and J. E. Parfrey, "Investigations on the penetration of hydrolyzed wheat proteins into human hair by confocal laser-scanning fluorescence microscopy," *J. Cosmet. Sci.* **51** 193-203 (2000)
- F. Saurenbach and B. D. Terris, "Electrostatic writing and imaging using a force microscope," *IEEE Trans. on Indus. Appl.* **28**, 256-260 (1992).
- D. K. Schroder, *Semiconductor Material and Device Characterization*, 3<sup>rd</sup> Edition, Wiley, Hoboken, 2006.
- J. R. Smith and J.A. Swift, "Lamellar subcomponents of the cuticular cell membrane of mammalian keratin fibers show friction and hardness contrast by AFM," *J. Microsc.* **206**, 182-193 (2002).
- G. D. Stern, B. D. Terris, H. J.Mamin, G. Rugar, " Deposition and imaging of localized charge on insulator surfaces using a force microscope," *Appl. Phys. Lett.* **53**, 2717-2719 (1988).
- B. D. Terris, J. E. Stern, D. Rugar and H. J. Mamin, "Contact electrification using force microscopy," *Phys. Rev. Lett.*, **63** 2669-2675 (1989).
- S. Thibaut and B. A. Bernard, "The biology of hair shape," *Int. J. Dermatol.* **44** S2-S3 (2005)
- S. Thibaut, O. Gailard, P. Bouhanna, D. W. Cannell, and B. A. Bernard, "Human hair shaped is programmed from the bulb," *Brit. J. Dermatol.* **152** 632-638 (2005)
- W. Tong, L. G. Hector Jr., H. Weiland, L. F. Weiserman, "In situ surface characterization of a binary aluminum alloy during tensile deformation," *Scripta Metall. Mater.* **36**, 1339-1344 (1997)
- G. Wei, B. Bhushan and P. M. Torgerson, "Nanomechanical characterization of human hair using nanoindentation and SEM," *Ultramicroscopy* **105** 155-175 (2005)
- C. Zviak (Ed.), *The Science of Hair Care*, Marcel Dekker, New York, 1986

## APPENDIX A

### Shampoo and conditioner treatment procedure

This appendix section outlines the steps involved in washing hair switches with shampoo and/or conditioner.

- Shampoo treatments

Shampoo treatments consisted of applying a commercial shampoo evenly down a hair switch with a syringe. Hair was lathered for 30 seconds, rinsed with tap water for 30 seconds, then repeated. The amount of shampoo used for each hair switch was  $0.1 \text{ cm}^3$  shampoo per gram of hair. Switches were hanged to dry in an environmentally controlled laboratory, and then wrapped in aluminum foil.

- Conditioner treatments

A commercial conditioner was applied  $0.1 \text{ cm}^3$  of conditioner per gram of hair. The conditioner was applied in a downward direction (scalp to tip) thoroughly throughout hair switch for 30 seconds, and then allowed to sit on hair for another 30 seconds. The switch was then rinsed thoroughly for 30 seconds. Switches were hanged to dry in an environmentally controlled laboratory, and then wrapped in aluminum foil.